NAVAL POSTGRADUATE SCHOOL
Monterey, California

DTIC
ELECTE
NOV 20 1986
S
B

THESIS

PARTICULATE SIZING IN A SOLID-PROPELLANT
ROCKET MOTOR USING LIGHT SCATTERING
TECHNIQUES

by

Kevin G. Horton

June 1986

Thesis Advisor: David W. Netzer

Approved for public release; distribution is unlimited

86 11 19 003

REPORT DOCUMENTATION PAGE

1a REPORT SECURITY CLASSIFICATION	1b RESTRICTIVE MARKINGS
Unclassified	

2a SECURITY CLASSIFICATION AUTHORITY	3 DISTRIBUTION/AVAILABILITY OF REPORT
	Approved for public release; distribution is unlimited
2b DECLASSIFICATION/DOWNGRADING SCHEDULE	

4 PERFORMING ORGANIZATION REPORT NUMBER(S)	5 MONITORING ORGANIZATION REPORT NUMBER(S)

6a NAME OF PERFORMING ORGANIZATION	6b OFFICE SYMBOL (If applicable)	7a NAME OF MONITORING ORGANIZATION
Naval Postgraduate School	Code 67	Naval Postgraduate School

6c ADDRESS (City, State, and ZIP Code)	7b ADDRESS (City, State, and ZIP Code)
Monterey, California 93943-5000	Monterey, California 93943-5000

8a NAME OF FUNDING/SPONSORING ORGANIZATION	8b OFFICE SYMBOL (If applicable)	9 PROCUREMENT INSTRUMENT IDENTIFICATION NUMBER
Air Force Rocket Propulsion Laboratory		

8c ADDRESS (City, State, and ZIP Code)	10 SOURCE OF FUNDING NUMBERS			
	PROGRAM ELEMENT NO	PROJECT NO FQ4611-86-X-0008	TASK NO	WORK UNIT ACCESSION NO
Edwards Air Force Base, California 93523				

11 TITLE (Include Security Classification)
PARTICULATE SIZING IN A SOLID-PROPELLANT ROCKET MOTOR USING LIGHT SCATTERING TECHNIQUES

12 PERSONAL AUTHOR(S)
Horton, Kevin G.

13a TYPE OF REPORT	13b TIME COVERED	14 DATE OF REPORT (Year Month Day)	15 PAGE COUNT
Master's Thesis	FROM _____ TO _____	1986, June	66

16 SUPPLEMENTARY NOTATION

17	COSATI CODES		18 SUBJECT TERMS (Continue on reverse if necessary and identify by block number)
FIELD	GROUP	SUB GROUP	Solid-Propellant; Rocket Motor; Light-Scattering; Particle Sizing

19 ABSTRACT (Continue on reverse if necessary and identify by block number)

An experimental investigation was conducted to determine the feasibility of introducing particles of a known mean diameter into a small solid propellant rocket motor and measuring the change in mean diameter across the exhaust nozzle. Light scattering profiles at small forward angles were recorded at the entrance and exit of the nozzle. The propellant utilized was nonmetallized and contained HTPB and ammonium perchlorate. Promising results were obtained for injections of polydispersions of glass beads and aluminum oxide particles.

20 DISTRIBUTION/AVAILABILITY OF ABSTRACT	21 ABSTRACT SECURITY CLASSIFICATION
☑ UNCLASSIFIED/UNLIMITED ☐ SAME AS RPT ☐ DTIC USERS	Unclassified

22a NAME OF RESPONSIBLE INDIVIDUAL	22b TELEPHONE (Include Area Code)	22c OFFICE SYMBOL
Prof. David W. Netzer	(408) 646-2980	Code 67Ne

DD FORM 1473, 84 MAR   83 APR edition may be used until exhausted
All other editions are obsolete

SECURITY CLASSIFICATION OF THIS PAGE

Particulate Sizing in a Solid Propellant Rocket
Motor Using Light Scattering Techniques

by

Kevin G. Horton
Captain, Canadian Armed Forces
BENG, Royal Military College of Canada, 1980

Submitted in partial fulfillment of the
requirements for the degree of
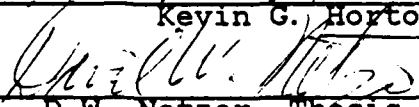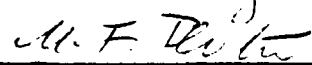
MASTER OF SCIENCE IN ENGINEERING SCIENCE

from the

NAVAL POSTGRADUATE SCHOOL
June 1986

Author: _____
Kevin G. Horton

Approved by: _____
D.W. Netzer, Thesis Advisor

_____
M.F. Platzer, Chairman,
Department of Aeronautics

_____
J.N. Dyer,
Dean of Science and Engineering

2

ABSTRACT

An experimental investigation was conducted to determine the feasibility of introducing particles of a known mean diameter into a small solid propellant rocket motor and measuring the change in mean diameter across the exhaust nozzle. Light scattering profiles at small forward angles were recorded at the entrance and exit of the nozzle. The propellant used was nonmetallized and contained HTPB and ammonium perchlorate. Promising results were obtained for injections of polydispersions of glass beads and aluminum oxide particles.

3

TABLE OF CONTENTS

LIST OF TABLES

LIST OF FIGURES

ACKNOWLEDGEMENTS

8

I. INTRODUCTION

The use of metals in solid propellant rocket motors has
brought directed attention to those aspects of performance
losses which are not observed with nonmetallized propel-
lants.   The mechanisms, which are detrimental to the effec-
tiveness of the rocket nozzle expansion process in
converting thermal to kinetic energy, are well known.   The
more important of these mechanisms are 1) a momentum loss
resulting from unburned metal particles not being acceler-
ated to the exhaust exit velocity (velocity lag); 2) an
energy loss due to the failure of metal particles to
completely transfer their thermal energy to the exhaust
stream before leaving the nozzle (thermal lag); 3) energy
loss through heat transfer from the exhaust products to the
nozzle; and, 4) a momentum loss through particle impingment
on the nozzle walls.

Mechanisms 1 and 2 are commonly grouped together under
the name of two phase flow losses and are often the largest
source of losses in a rocket's specfic impulse and perform-
ance [Ref. 1].   Methods for predicting two phase flow losses
have been created and are commonly used as an integral part
of rocket motor and propellant design.   One of the most
important variables in the prediction of two phase flow
losses is the size of condensed metal particles in the
nozzle.   Hence, it follows that any performance predictions
depend on the ability to accurately determine the size of
particles in the motor and nozzle environment.

Analytical computer programs, which attempt to predict
performance for solid rocket motors, such as the Improved
SPP (Solid Performance Program) [Ref. 2] are semi-empirical
due to the lack of understanding of the fundumental
processes.   The two-phase flow losses are based on particle

size data from collected exhaust samples of small motors. Hermsen [Ref. 3] improved the SPP prediction code by adding an empirical approach using linear and nonlinear least square methods, but the improvement still required correlating collected particle size data . Price [Ref. 4] provides a good summary of the combustion behavior of metallized propellants in the rocket motor environment, and shows that experiments must be carried out to determine how particle sizes vary in the actual flow environment in order to truely validate the models for two phase flow losses.

At the Naval Postgraduate School Combustion Laboratory an investigation was initiated to probe the use of light scattering techniques to obtain particle size data across the exhaust nozzle of a small rocket motor [Ref. 5, 6]. Forward light scattering provides a viable method for collecting data and essentually does not disrupt the motor environment. Utilizing an approach presented by Buchele [Ref. 7] the diffraction of light scattered by particles are analyzed in order to obtain the volume to surface mean diameter, D_{32}.

A validation of the techiques in use was conducted by Rosa [Ref. 8] with good success outside the motor. However, combustion light at the wavelength of the transmitted light and/or multiple scattering greatly hampered the light scattering measurements within the motor.

The purpose of this investigation was to modify the apparatus developed in previous efforts in an attempt to make measurements of the changes in mean particle size across the motor port and across the exhaust nozzle. In most cases the particle sizes leaving the propellant surface are unknown., and are not directly related to propellant properties. In order to know the initial particle sizes a different approach was taken. A nonmetallized propellant with an internally burning grain was used and aluminium

10

oxide particles of a known size distribution were introduced at the motor head-end.

II. THEORETICAL BACKGROUND

Van de Hulst [Ref. 9] discusses in detail the theory involved in the light scattering properties of particles of arbitrary size and refractive index as first proposed by Mie. The Mie equation for light scattering, although applicable to all situations, is very complex and difficult to use in data reduction due largely to the inclusion of Legendre polynomials and spherical Bessel functions.

Light scattering investigations subsequent to Mie's theory determined that alternate, less complicated, theories such as Rayleigh scattering and Fraunhofer diffraction could be utilized when the particles were much smaller or larger, respectively, than the wavelength of the incident light.

The present investigation was concerned primarily with two-phase flow losses. These losses depend primarily upon the larger (3-20 micron) particles in the exhaust, rather than the larger quantity of very small (less than 2 micron) particles. These particles have diameters significantly greater than the wavelength of light, and hence, their characteristics are adequately described by Fraunhofer diffraction.

Fraunhofer diffraction for a monodispersion is given by the equation

$$I(\theta) = [2J_1(\alpha\theta)/(\alpha\theta)]^2$$

$I(\theta)$ is the ratio of intensity of scattered light at some angle (θ) to the intensity of scattered light at theta equal to zero degrees

$J_1(\alpha\theta)$ is a first order Bessel function, and

12

$\alpha = \pi D / \lambda$ is the particle size parameter for diameter D and wavelength of light (λ).

Particle size is then determined by the angular distance of subsequent maxima and minima in the diffraction pattern.

Dobbins, et al [Ref. 10] found that, although Fraunhofer diffraction techniques were not able to determine polydispersion size distributions, the mean diameter could be determined by the angular distribution of diffracted light. The equation for the polydispersion volume to surface mean diameter is

$$D_{32} = \int_0^{Dmax} N_r(D) \, D^3 dD \; / \; \int_0^{Dmax} N_r(D) \, D^2 dD$$

$N_r(D)$ is a distribution function describing the proportion of particles with diameter D in the sample. It is noteworthy that Dobbins made use of the Upper Limit Distribution Function as proposed by Mugele and Evans [Ref. 11]. Buchele [Ref. 7] has recently summerized the experimental techniques for determining particle size by measurements of diffractively scattered light. In his report Buchele presents a function which closely expresses the curves given in the study by Dobbins, et al.

$$I(\theta) = EXP - (.57\alpha\theta)^2$$

The above expression was used in the present investigation to reduce data and obtain a mean diameter, D_{32}.

III. EXPERIMENTAL APPARATUS

A. INTRODUCTION

A photograph of the complete apparatus is presented in Figure 3.1. The major modifications to the motor and apparatus used in previous investigations were threefold;

- The rocket motor mount was modified in order to fire the rocket vertically, vice horizontally as before,

- Three inches were added between the rocket motor windows and the nozzle to allow the two laser optical systems to be used directly on top of each other, and,

- A new ignition port was positioned on the body of the motor to light the rear face of the propellant. The igniter port used previously was used for a particle feeder to introduce particles into the head-end of the motor.

B. ROCKET MOTOR

The motor components are displayed in a photograph in Figure 3.2, and represented in schematic form in Figure 3.3. The particle feeder components are shown in Figure 3.4, and also presented in a schematic in Figure 3.5. The feeder essentially consisted of three parts; a hopper and feeding tube leading into the rocket motor, a solenoid actuated spoon which allowed the investigator to open the hopper and introduce particles into the motor, and finally a three-ported disk which induced the particles into a spreading profile as they entered the motor cavity.

The propellant grain was two inches in diameter and one inch in length with a web thickness of .725 inches. The grain was cylindrically perforated in order to obtain a plateau burning design. A $BKNO_3$ igniter was used and ignition was accomplished by heating a resistance wire with a 12 VDC source.

14

The copper exhaust nozzle used in previous reports [Ref. 6] was modified for use in this experiment by means of developing an insert that could be changed to vary the throat diameter. This modification did not alter the operation of the nozzle or motor in any way but simply provided a convenient and economical way to change the nozzle throat diameter. Specifications and a schematic of the nozzle with insert are shown in Figure 3.6.

C. LIGHT SCATTERING APPARATUS

The apparatus shown in Figures 3.1 and 3.6 was essentially the same as used in reference 8. The light sources used through the exhaust and motor cavity were 8 and 5-milliwatt helium neon lasers, respectfully. Specifications are given in Table II. The lasers were mounted on two parallel optic benches, one for the beam passing through the exhaust, and the other for the beam passing through the motor cavity approximately three inches in front of the nozzle entrance. The motor cavity optical bench was mounted on a hinged base in order to allow it to be swung into position for firing, and out of position for ease of equipment set up and take-down.

The laser used in the exhaust was expanded and collimated in order to encounter a maximum of particles in the sparsely populated exhaust. The incident beam of each laser was intercepted by a physical stop placed immediately in front of the narrow pass filter that was used to eliminate extraneous light. The narrow pass filters, 2.3 centimeters diameter in the motor cavity and 5.08 centimeters diameter in the exhaust, were placed 30.5 centimeters from the motor centerline for the exhaust beam and 11.5 centimeters from the motor centerline for the motor cavity beam. This resulted in a maximum angle for collecting scattered light of 4.8 degrees in the exhaust and 6.0 degrees in the motor

15

cavity. Immediately following the narrow pass filter a condensing lens, with a diameter of 5.08 centimeters, was placed in both beam paths. Both lenses had a focal length of 50 centimeters and were alligned in order to focus the diffracted light from particles onto a linear array of photodiodes. When measurments were taken during a firing the diode arrays were positioned 1.0 centimeter below the undisturbed focussed beam. Scattered light between .02 and .07 radians was incident on the array. In the current apparatus an eight inch stainless steel tube was positioned around the exhaust stream in order to redirect the exhaust away fron the optical bench.

D. DATA ACQUISITION AND REDUCTION

Details of the data acquisition system are presented in reference 5. The system controller was an HP 9836S computer and an HP 6942A multiprogrammer was used for rapid A/D conversion and storage.

The 9836S has two internal disk drives which were used to store data after acquisition. Eight consecutive scans of the photodiode array in the exhaust were made, followed by four motor cavity scans. The point during the firing when data was taken was controlled by the acquisition system. This was accomplished by monitoring the motor chamber pressure and specifying a time delay after steady state operation was obtained.

The multiple scans of each array provided a statistically more valid measures of particle size than obtainable with a single scan.

Data reduction was accomplished using the method detailed in reference 8. The method consists of an iterative graphics technique used to fit a theoretical profile (for a specified D_{32} based on a selected angle (θ_1) and corresponding intensity (I_1) at that angle) to an

16

experimentally obtained profile. The approximate equation
for a polydispersion curve as presented by Buchele [Ref. 7]
is

$$I(\theta)=EXP-(.57\alpha\theta)^2$$

When applied between two different positions on the
diode array the following equation is obtained:

$$I_2=I_1EXP-[(\theta_2^2-\theta_1^2)(.57\alpha)^2]$$

Therefore, when a series of θ_2's are choosen a series of
I_2's are generated, and then a theoretical profile of I vs
θ is superimposed on the experimental data passing through
the point I_1 and θ_1. If the theoretical curve does not fit
the experimental data, other values of D_{32} can be selected,
and new theoretical curves generated. Therefore, as
described in reference 8, the mean particle size is based
upon fitting an approximate (although quite accurate) theo-
retical profile for a polydispersion to the profile obtained
experimentally over a small range of scattering angles.
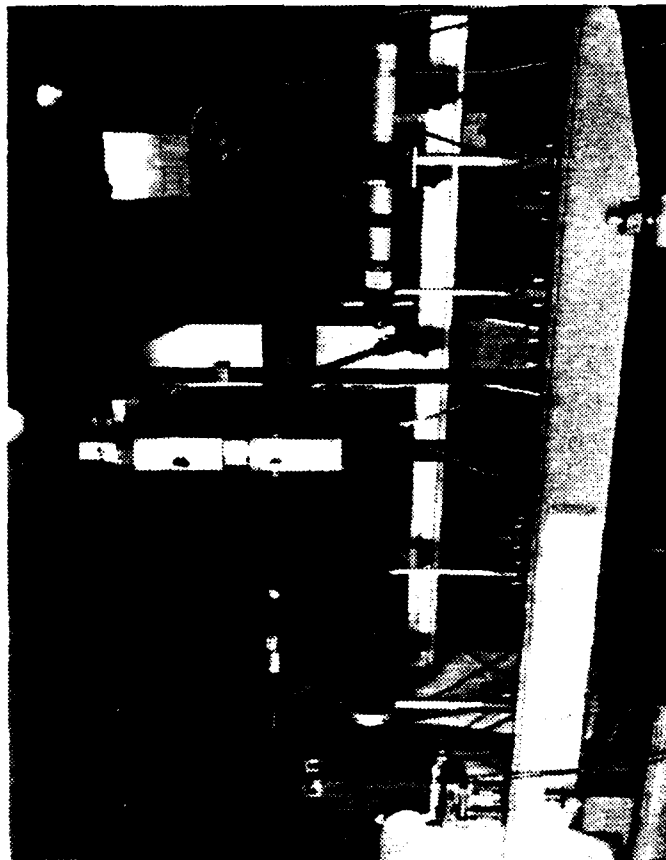
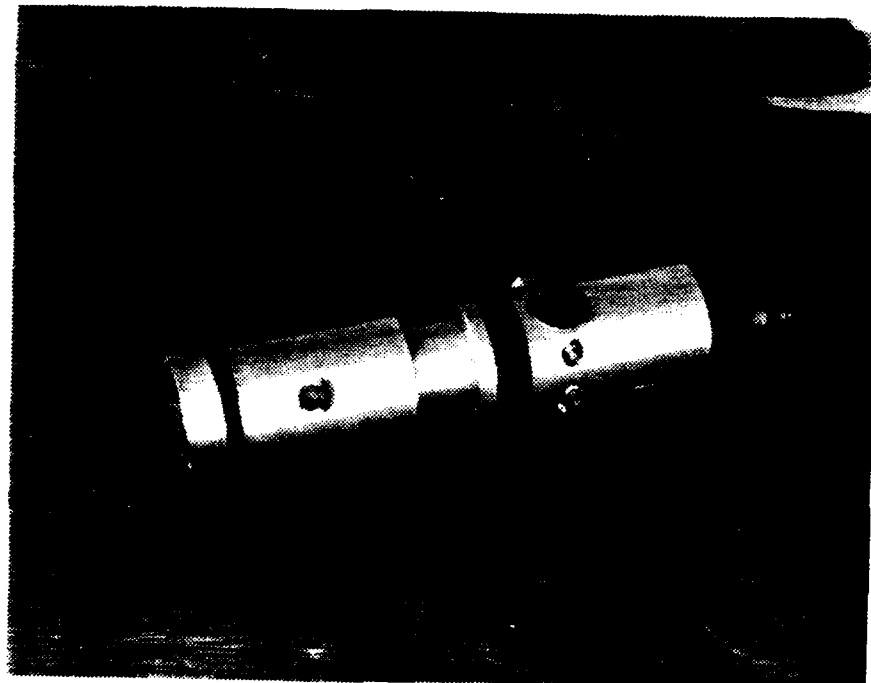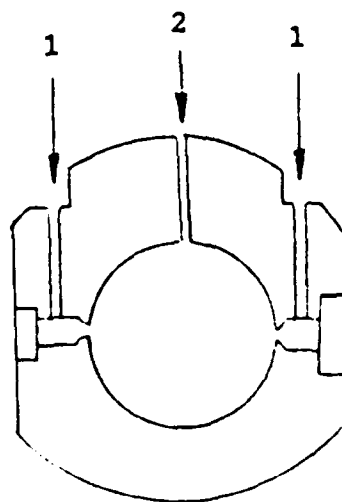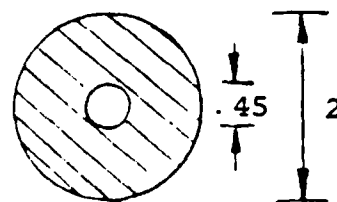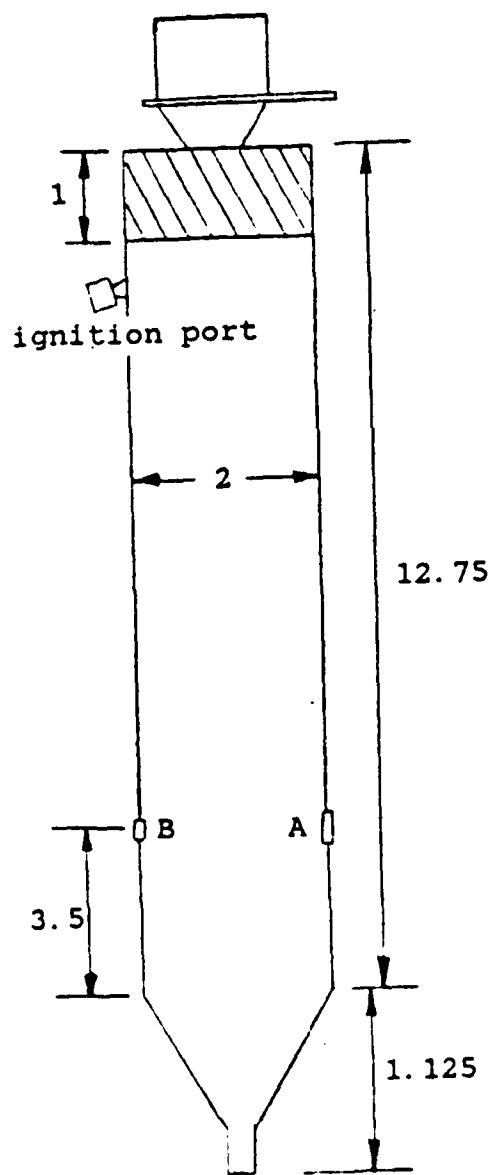Figure 3.1   Photograph of Complete Experimental Apparatus.

Figure 3.2   Photograph of Motor Components.

ignition port

1 - Nitrogen Purge

2 - Pressure Transducer

A - Large Window (.30)

B - Small Window (.15)

Note: all dimensions in inches

Figure 3.3   Schematic Diagram of Assembled Motor.

20

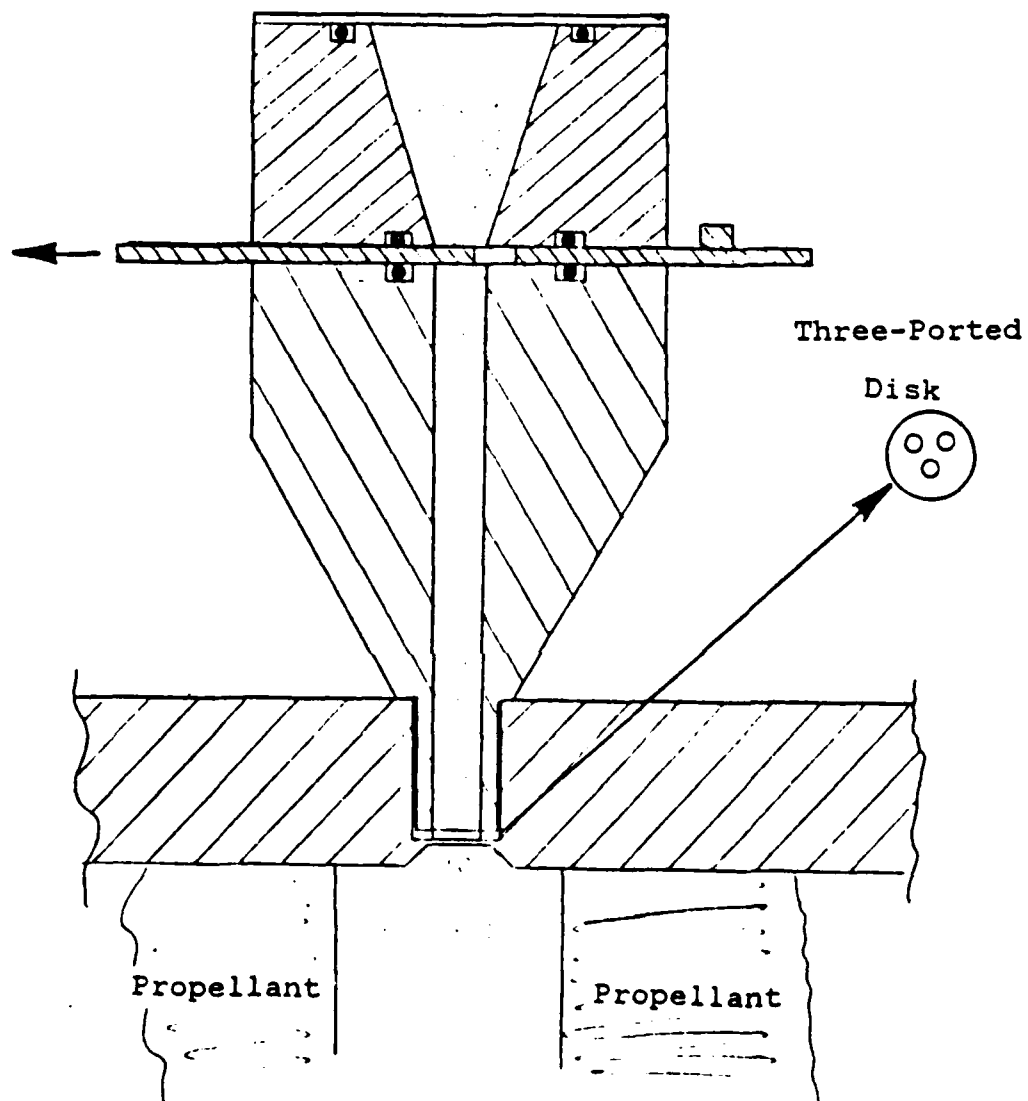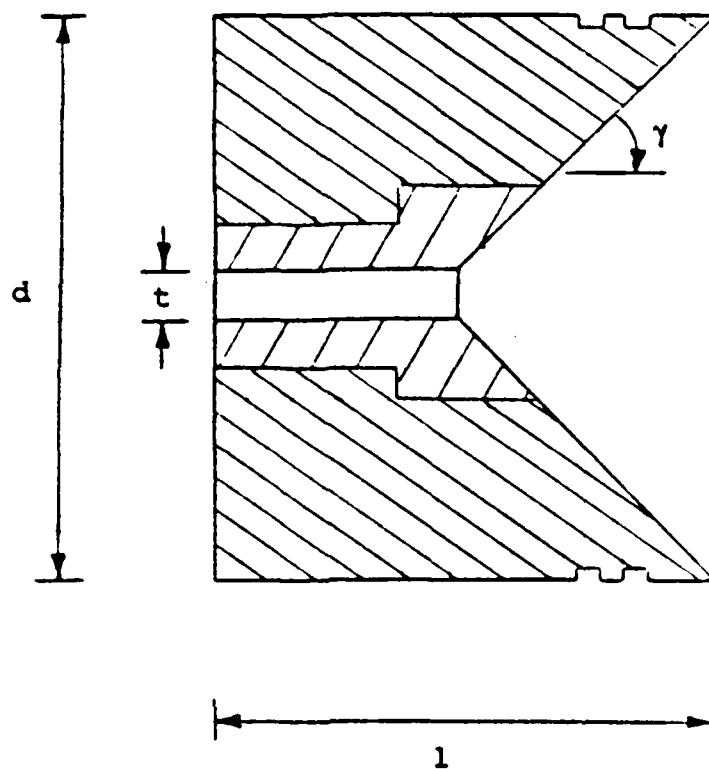Figure 3.4   Photograph of Particle Feeder Components.

21

Figure 3.5   Schematic Diagram of Assembled Particle Feeder.

TABLE I
NOZZLE SPECIFICATIONS

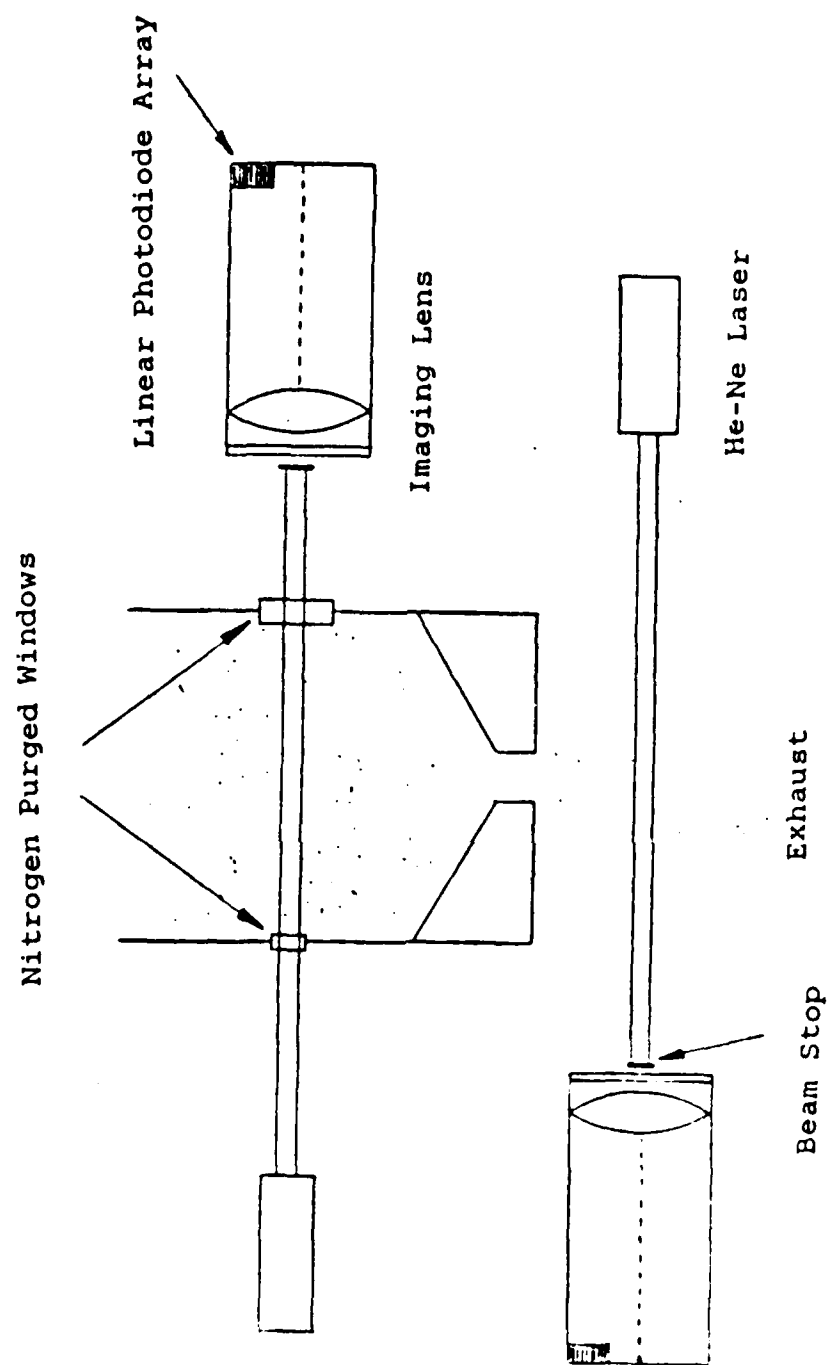| Description	Copper Nozzle
Outside Diameter (d, inches)	2.125
Length (l, inches)	1.25
Throat Diameter (t, inches)	.15
Slope Angle (γ, degrees)	45

23

Figure 3.6   Schematic Diagram of Light Scattering Appartus.

TABLE II
LASER SPECIFICATIONS

A. Helium-Neon Laser (Exhaust)

    1. Manufacturer   Spectra-Physics

    2. Model: 147

    3. Type: He-Ne Class IIIB

    4. Output Power: 8 mWatt

    5. Beam Diameter: .92 mm

    6. Beam Divergence: .87 nrad.

B. Helium-Neon Laser (Motor Cavity)

    1. Manufacturer: Uni-Phase

    2. Model: 1305P

    3. Type: He-Ne Class IIIB

    4. Output Power: 5 mWatt

    5. Beam Diameter: .81 mm

    6. Beam Divergence: 1.00 mrad.

IV. RESULTS AND DISCUSSION

A. INTRODUCTION

The purpose of this investigation was to measure the change in mean particle size across the exhaust nozzle of a small solid propellant rocket. An inherent problem in any particle sizing experiment of this type is the formation of agglomerates and accumulates as particles concentrate on the propellant burning surface. Unique to this investigation was the attempt to develop a workable method of introducing aluminum oxide (or other metal), of a known mean diameter, into a motor burning non-metallized propellant. This additional step, although recognized as being quite different in terms of particle, burning surface and gas flow interactions, produces controls which could potentially provide valuable information about the 'life sequence' of particles in solid rocket motors.

B. MOTOR SIMULATION

In order to properly test the proposed method of introducing particles into an ignited motor, a scaled down Plexiglas model of a rocket motor was manufactured and is shown in Figure 4.1. Nitrogen was used to pressurize the model and was passed through a small (one half inch inside diameter) gasoline filter in an attempt to simulate hot gases rising from a burning propellant surface. Once the model chamber pressure had been set, a single ported spoon could be alligned to allow aluminum oxide particles from the hopper to fall (via gravity) through the feeding tube and into the rocket body. Photographs of high speed movies (Figure 4.2 and 4.3) taken just aft of the gasoline filter

26

verified the applicability of the proposed method in consideration to both uniformity and distribution of the falling particles. Although high speed movies of particles falling within the real motor could not be taken due to illumination problems, holograms of the particles (Figure 4.4) in cold flow in the motor also showed good distribution and uniformity. At this time in the investigation the importance of having spherical particles was discovered. In all the previous test runs, spherical glass beads were used with good success, but when 20 micron aluminum oxide grit was used, the non-spherical characteristic prevented the particles from freely falling under any circumstances. Fortunately, spherical aluminum oxide particles with a distribution of 1-100 microns were obtained, which, after screening, provided particles with a 1-44 micron distribution for use in the investigation.

C. SYSTEM CALIBRATION

The apparatus was calibrated by Rosa [Ref. 8] using the standard calibration procedure as detailed by Harris [Ref. 5]. The apparatus was recalibrated in this study as a result of the modification done to fire the rocket vertically instead of horizontally. A calibration involved passing the laser beam through a Plexiglas container holding a suspension of either polystyrene spheres or glass beads in water. The photodiode array was alligned so that the incident laser beam was positioned on the number one diode. Then the diode array was dropped down one centimeter, allowing the array (2.56 centimeters in length) to measure the intensity of light scattered at angles from .02 to .07 radians.

A polydispersion sample of polystyrene spheres, with a D_{32} of 10.2 microns, was initially used for the calibration. The results are presented in Figures 4.5 and 4.6. The

27

results show good agreement with the actual mean diameter of the sample. Additional calibrations were also conducted within the motor cavity with the window nitrogen purge in operation in order to determine if it altered the light scattering in any way. The results, which showed no discernable effect, are presented in Figures 4.7 and 4.8.

A second polydispersion sample of glass beads with a D_{32} of 25 microns, was also used for calibration and resulted in light scattering profiles consistent with particles of less than 15 microns in diameter until adjustments were made to the measuring angles of the scattered light. Knowing that large particles diffract light at small angles the photodiode array was lowered only .5 centimeters below the main beam and the calibration was repeated with good results (Figure 4.9). This procedure resulted in the range of angles measured becoming .01 to .06 radians.

Much has been written about bi-modal distributions of particles in solid propellant rocket motor exhausts. It is the larger particles that are of interest in two-phase calculations. Although a true bi-modal distribution is difficult to produce, the effects of a high concentration of small particles in a known distribution of larger particles could be examine. To this end, a calibration using polystyrene spheres, with a distribution of 3 to 6 microns and D_{32} of 4.8 microns, was completed with the results presented in Figure 4.10. A second light scattering profile, Figure 4.11, was then obtained when polystyrene spheres with a D_{32} of 0.9 microns in very high concentration were added to the 4.8 micron sample. As shown by the two light scattering profiles, although the smaller particles have an effect on the D_{32} of the total distribution, the larger particles have the greatest and most predominate effect on the resultant D_{32}.

D. MOTOR FIRING DATA

The propellant used in this investigation was a nonme-
tallized composite propellant consisting of an inert binder,
(15% HTPB) and an oxidizer (85% ammonium perchlorate). When
burned at 200 psi the propellant would produce a theoretical
chamber temperature of 2860 K. Therefore, two different
available spherical particle compositions with acceptable
melting temperatures were tested in firing applications:
glass beads (melting temperature of approximately 1700 K)
and aluminum oxide (melting temperature of 2320 K).

1. **Glass Beads**

Three tests were conducted where glass beads, with a
distribution of 1 to 37 microns and a calculated D_{32} of 25
microns, were fed into the ignited motor. The motor firing
data and a summary of particle size measurements across the
nozzle are presented in Table III. These results are also
presented in Figures 4.12 through 4.17. The light scat-
tering measurements, although not in precise agreement, did
point out a definite trend towards a reduction in mean diam-
eter across the exhaust nozzle. Additionally, it is inter-
esting to note the wide variation in chamber pressures (310
to 600 psi) when glass bead particles were fed into the
motor, especially when the chamber pressure of the base
propellant without particles added never rose above a pres-
sure of 230 psi.

2. **Aluminum Oxide**

Five tests were conducted where aluminum oxide, with
a distribution of 1 to 44 microns and a calculated D_{32} of 30
microns, were fed into the ignited motor. The firing data
and a summary of the particle size measurements are
presented in Table IV and V. These results are also
presented in Figures 4.18 through 4.27. The light scat-
tering diameter measurements were fairly consistent within
each test run, but seemed significantly smaller than the

29

calculated diameters from SEM evaluations of collected particles. Some possible contributing factors for these variations are that; 1) particles can continue to run out of the particle feeder onto the nozzle (where they were collected for SEM analysis) after the propellant has completed burning, 2) the potential for large agglomerates to form has increased due to combustion moisture from the burning propellant, 3) the exhaust tube, primarily used to redirect the rocket exhaust away from the optical test bench, was positioned at such an acute angle so as to not obtain a truely representative sample (reflected in the relatively small sample number), and 4) a polydispersion of 1-44 microns is too broad a distribution to properly use in an investigation of this nature. It is felt that a polydispersion of not more than 20 microns with a maximum particle size of 25 or 30 microns should be used in future studies.

The Al_2O_3 particle size appeared to increase slightly across the nozzle, in contrast to the glass beads.

Finally, a wide variation in chamber pressures was again obtained when aluminum oxide particles were fed into the motor.

3. <u>System Problems</u>

In attempting to design a realistic system for feeding particles into a rocket motor, an obvious concern was in determining the residence time of the particles in the motor. In the burning of a metallized propellant, the metal will become molten as it reaches the burning surface and, whether it agglomerates or not, it will be molten as it enters the gas flow. In this investigation, although the aluminum oxide particles were not molten as they entered the gas flow, it was assumed that they could become molten, depending on their melting temperature and residence time, prior to completing their flow over the burning propellant

30

grain. The residence times for pressures of 250,400 and 600 psi for the distances; 1) to the end of the propellant grain, 2) to the windows, and 3) to the nozzle throat, are presented in Table VI. The residence times of the particles within the grain were quite short. However assuming that the gas temperature was not reduced significantly (by heat transfer to the uninsulated walls) within the motor, sufficient time (approximately 50 msec) existed for the glass beads and aluminum oxide particles to become molten before entering the exhaust nozzle.

A very noticeable problem in the present system was the very wide fluctuations in chamber pressures during test runs with essentially the same operating conditions. In addition to an increased pressure, the pressure traces indicated a reduction in overall burning time as expected for an increased burning rate for the propellant. These changes are believed to be the result of particles impinging on the burning propellant surface and conducting additional heat back into propellant. This situation of impingment is undoubtedly enhanced by the relatively small grain port diameter and by the fact that the port was often cut unintentially at a small angle to the vertical. On the surface, the solution to this problem would appear to be to merely increase the size of the hole cut in the propellant. However, this would result in a significant reduction in the burn time. Therefore, the problem would be best solved with an overall increase in the rocket motor's internal dimensions and, subsequently, an increase in the propellant's outside diameter.

As stated earlier, moisture from the burning propellant periodically can invalidate a test run by causing particles to stick together and block the feeding tube, or pass through the motor as very large agglomerates. Although unfortunate, this problem would seem to be unavoidable in

31

the present system and realistically presents only a minor
problem.
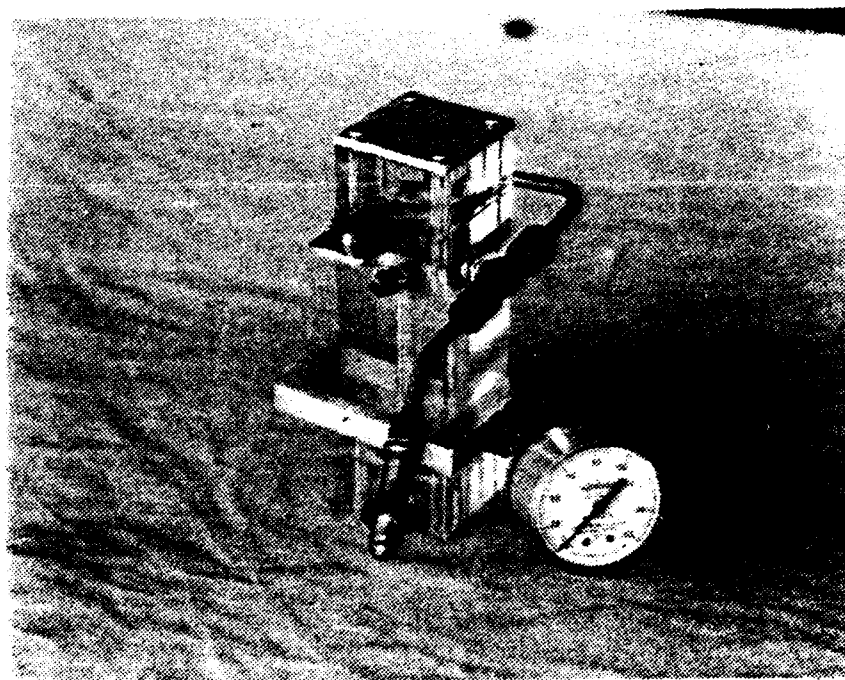
Figure 4.1   Photograph of Plexiglas Rocket Model.

33
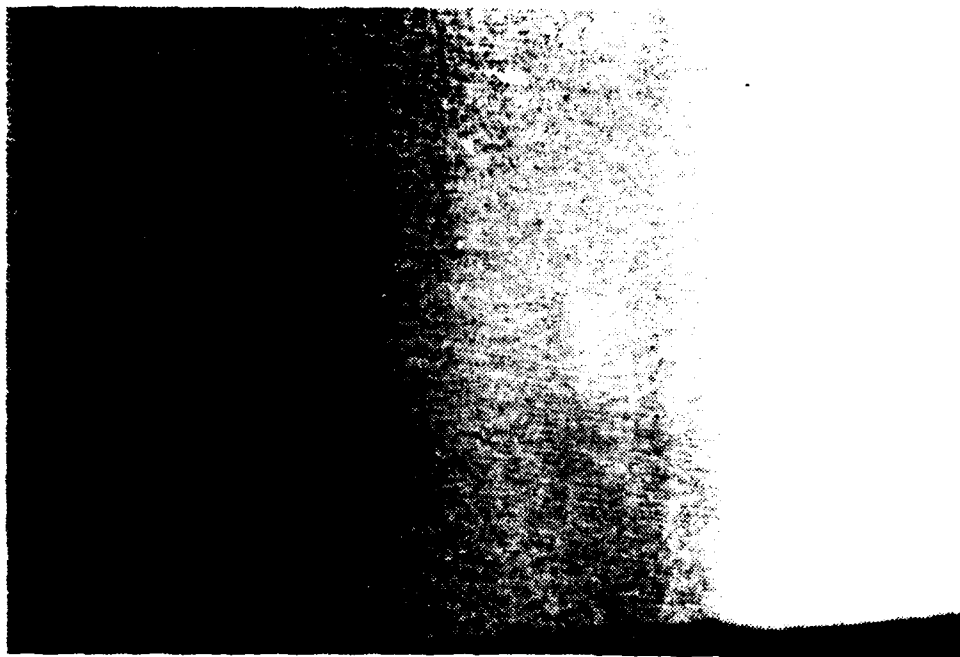
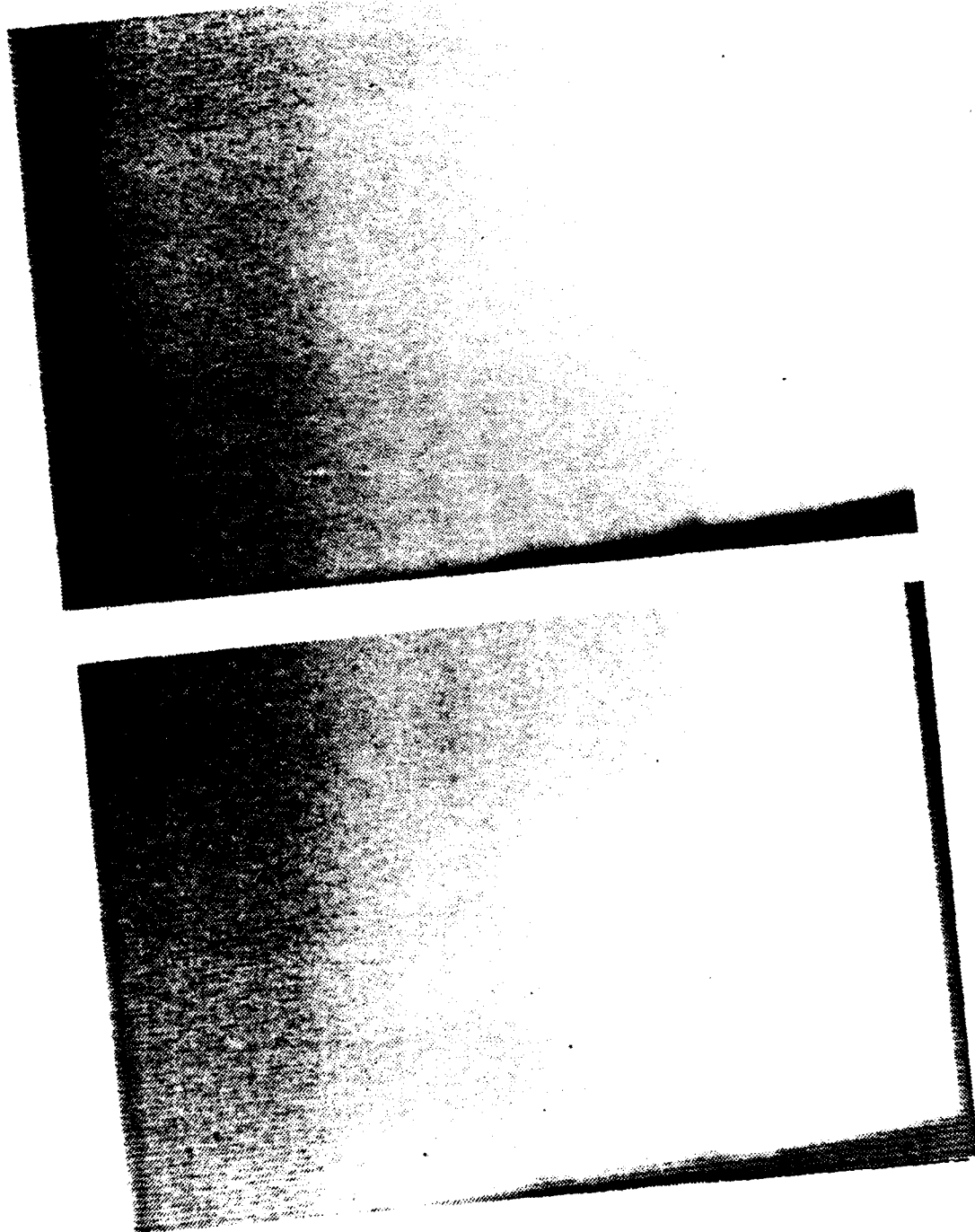Figure 4.2   Photographs of Particles in Plexiglas Model.
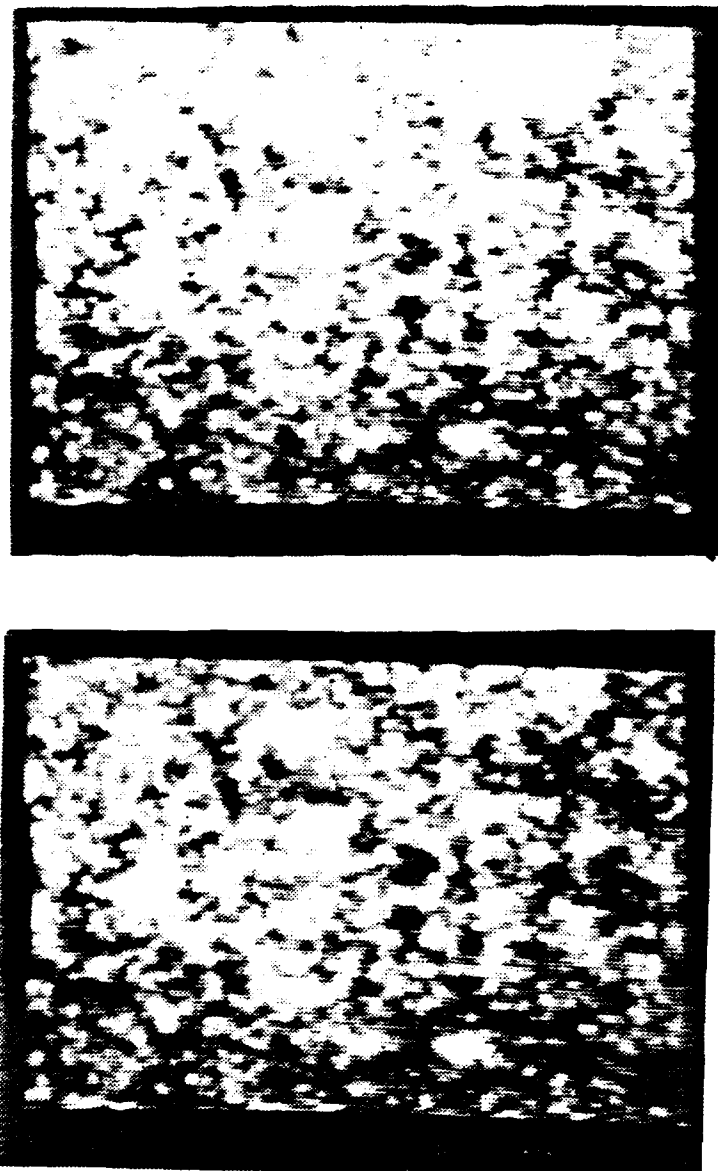
34

Figure 4.3   Photographs of Particles in Plexiglas Model.

35

Figure 4.4   Photographs of Reconstructed Holograms
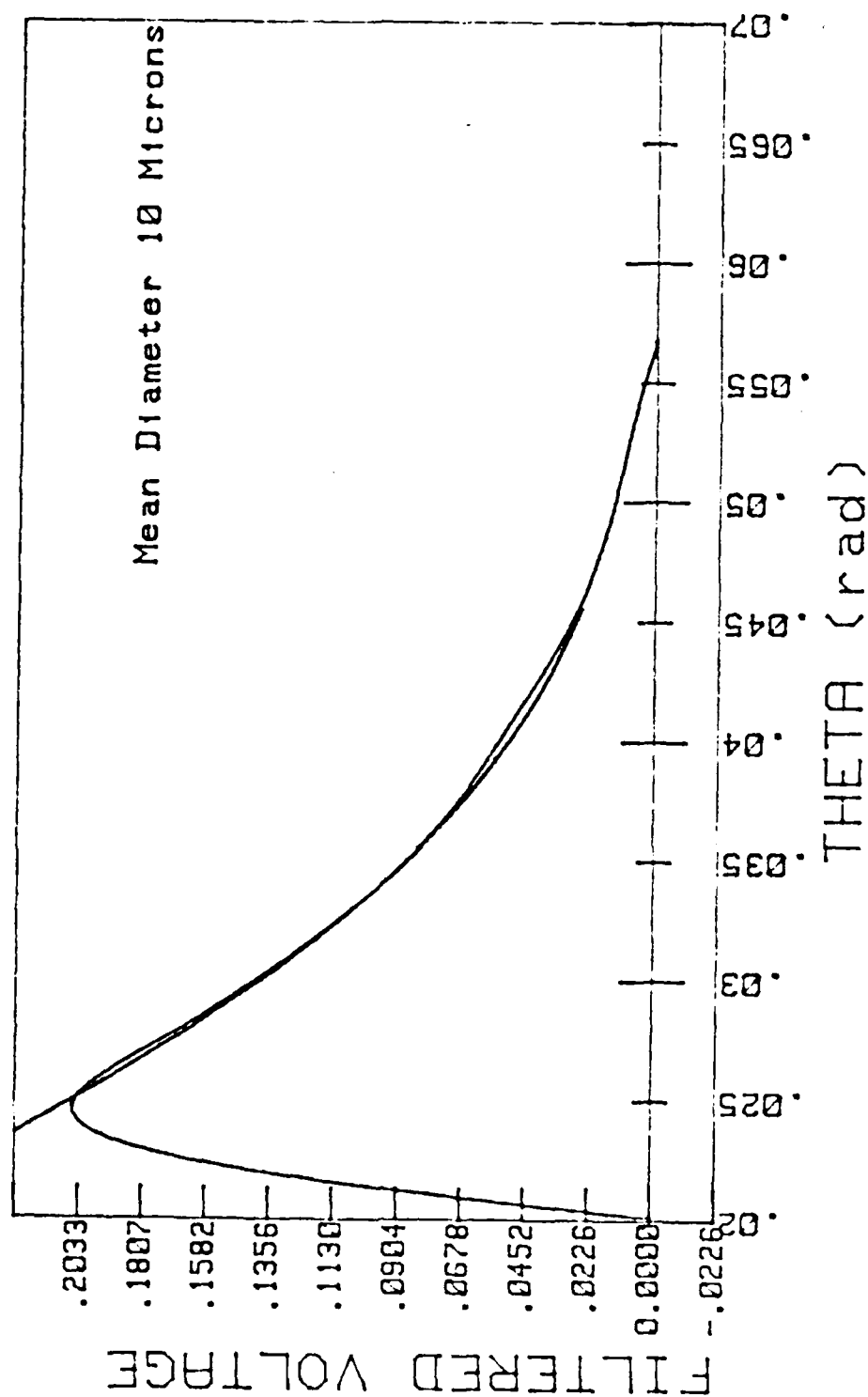of Particles in Rocket Motor with Cold Flow.

Figure 4.5   Motor Calibration with 10.2
Micron Polystyrene Spheres.
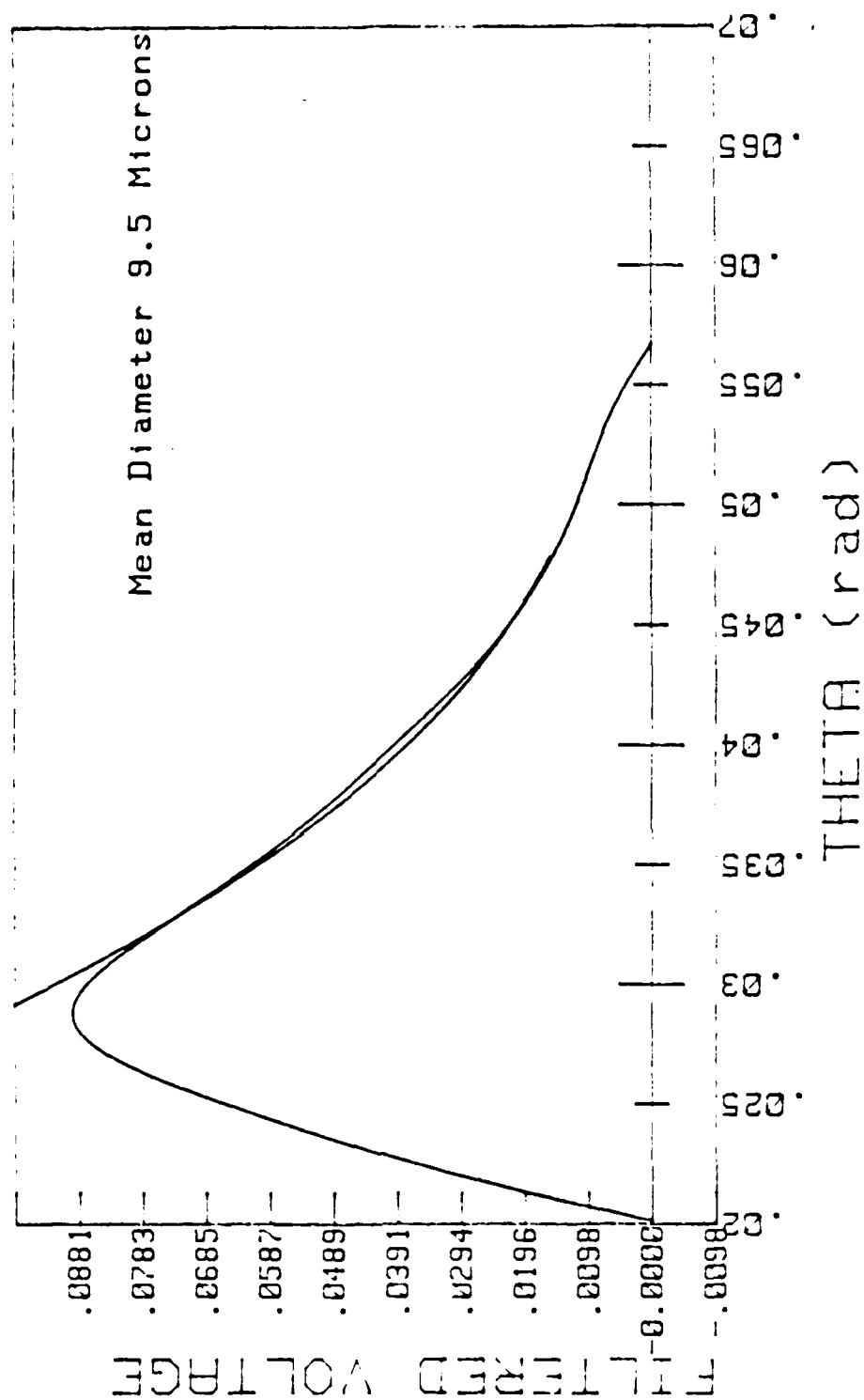
Figure 4.6   Exhaust Calibration with 10.2
Micron Polystyrene Spheres.

38

CURVE FIT RESULTS
INTENSITY vs. THETA

Mean Diameter 10 Microns
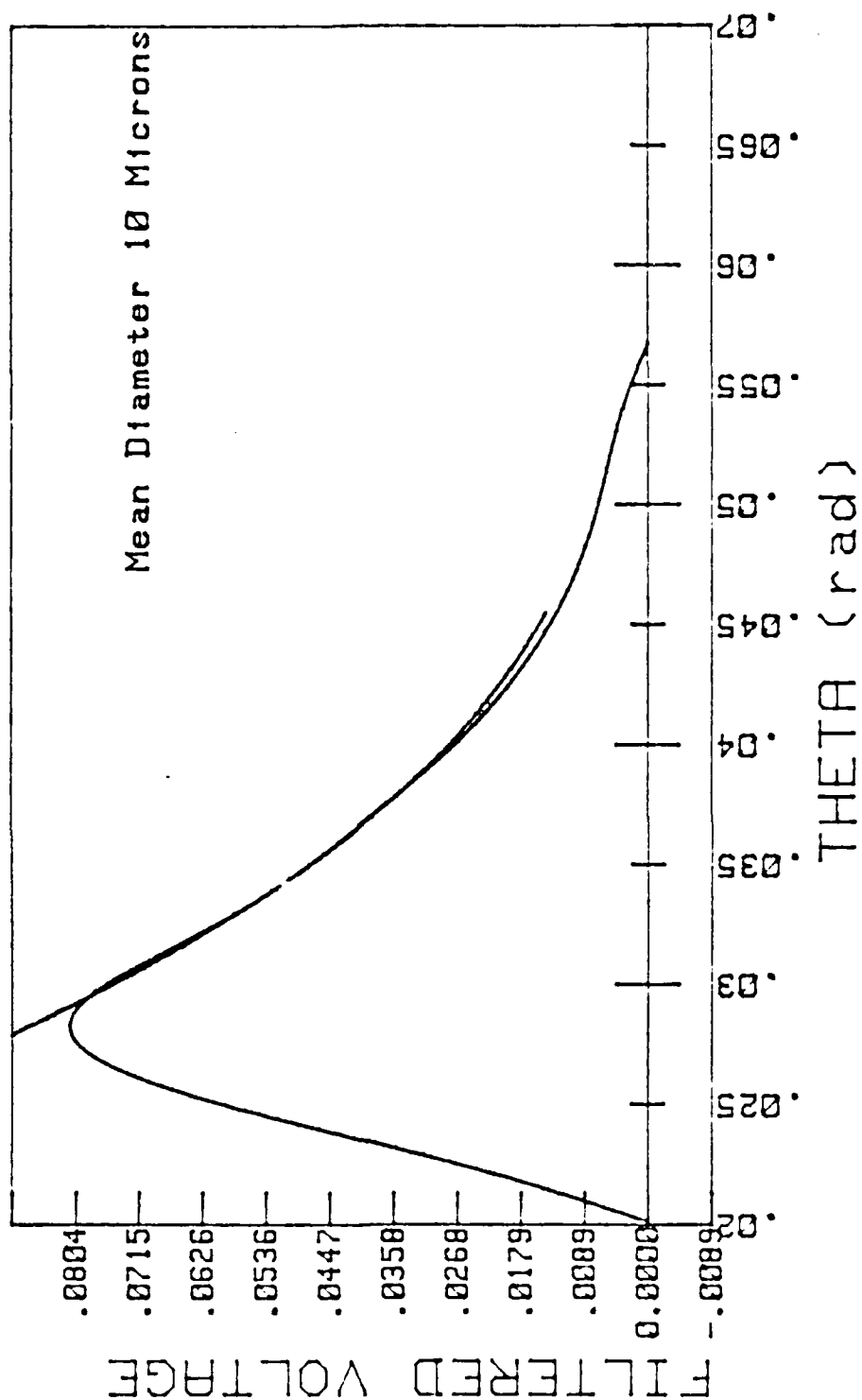
Figure 4.7   Calibration with 10.2 Micron Polystyrene Spheres.

39
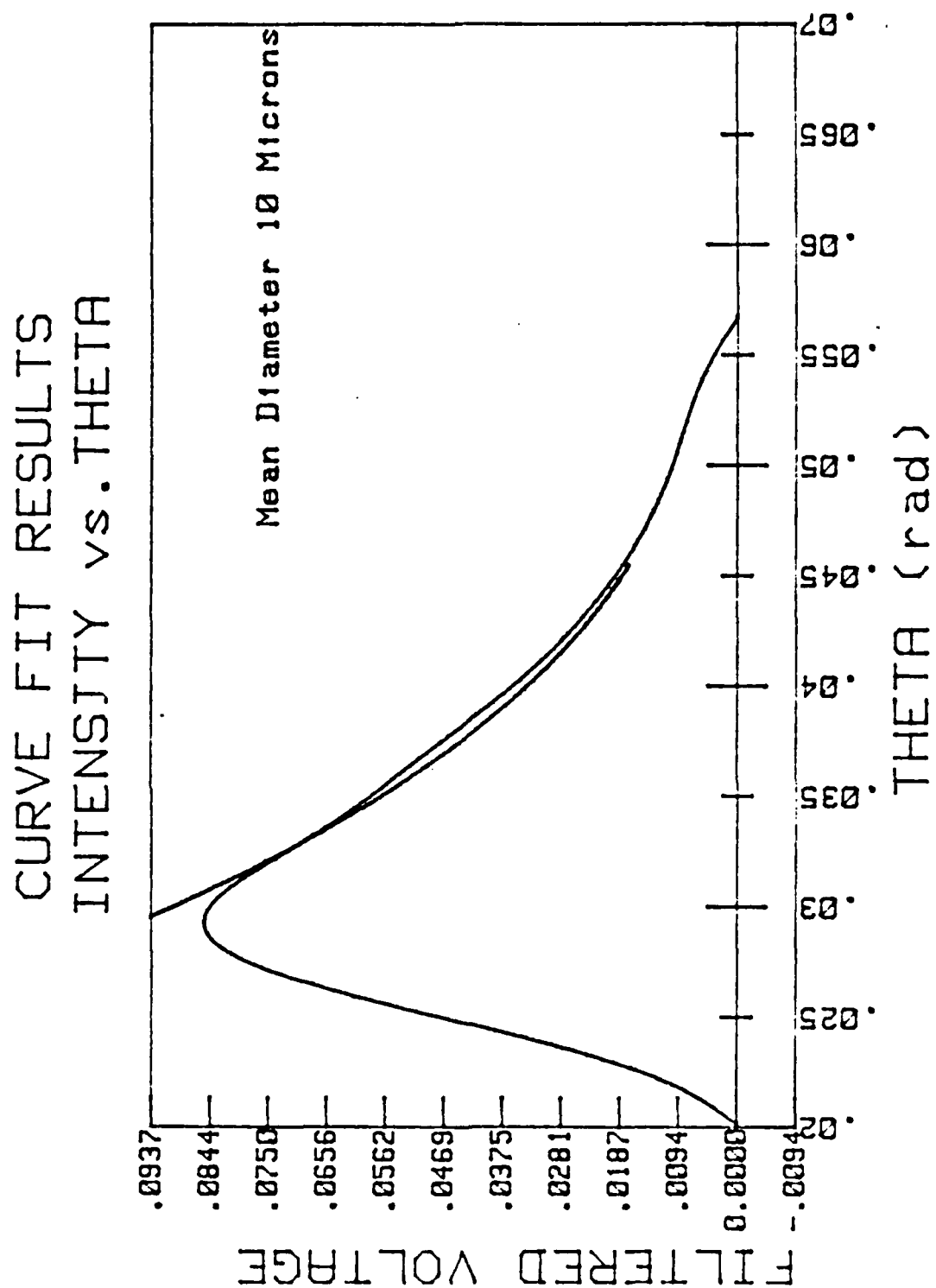
Figure 4.8   Motor Calibration with 10.2 Micron Polystyrene
Spheres and Nitrogen Purge.

40
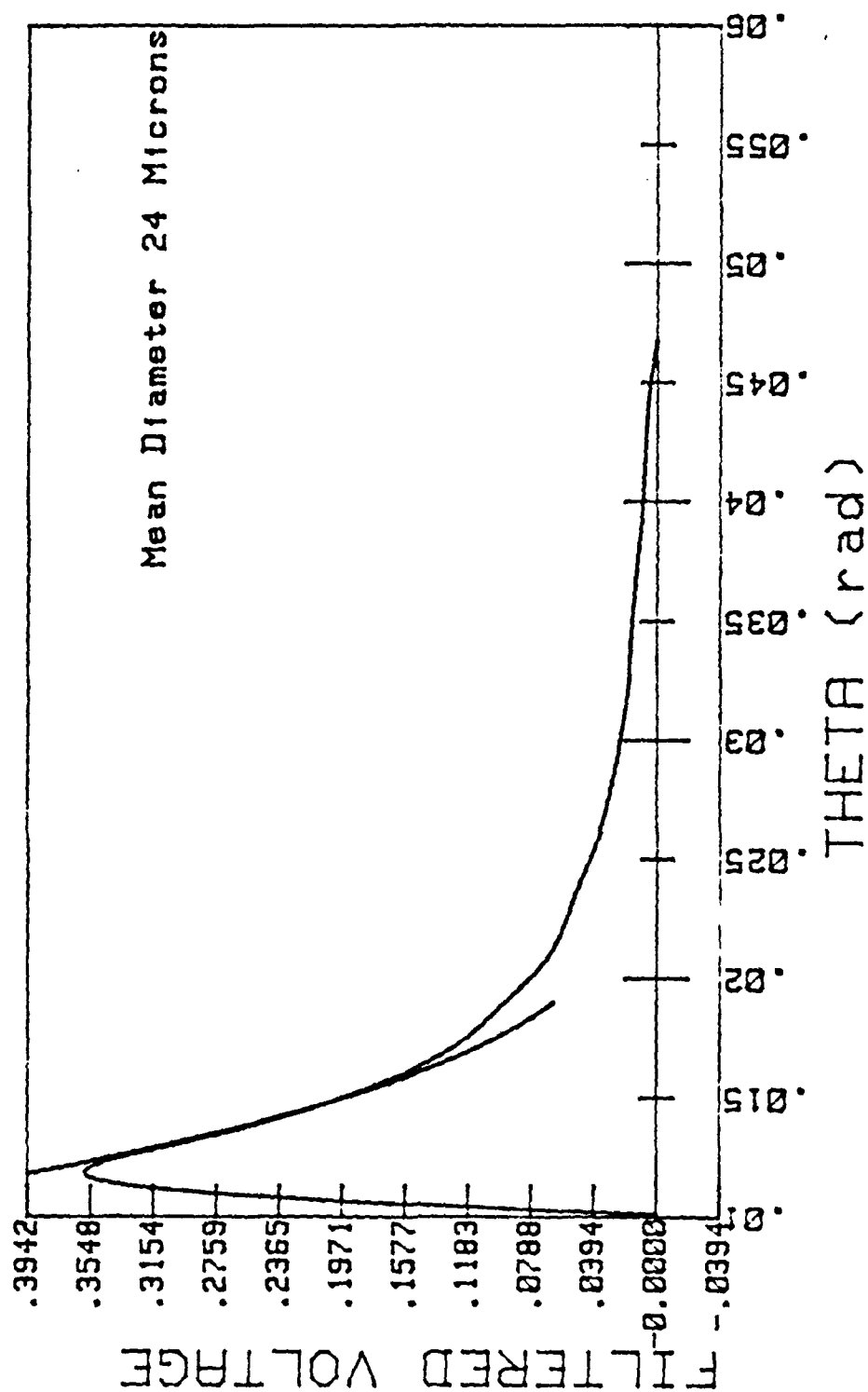
Figure 4.9   Calibration with 25 Micron Glass Beads.

41
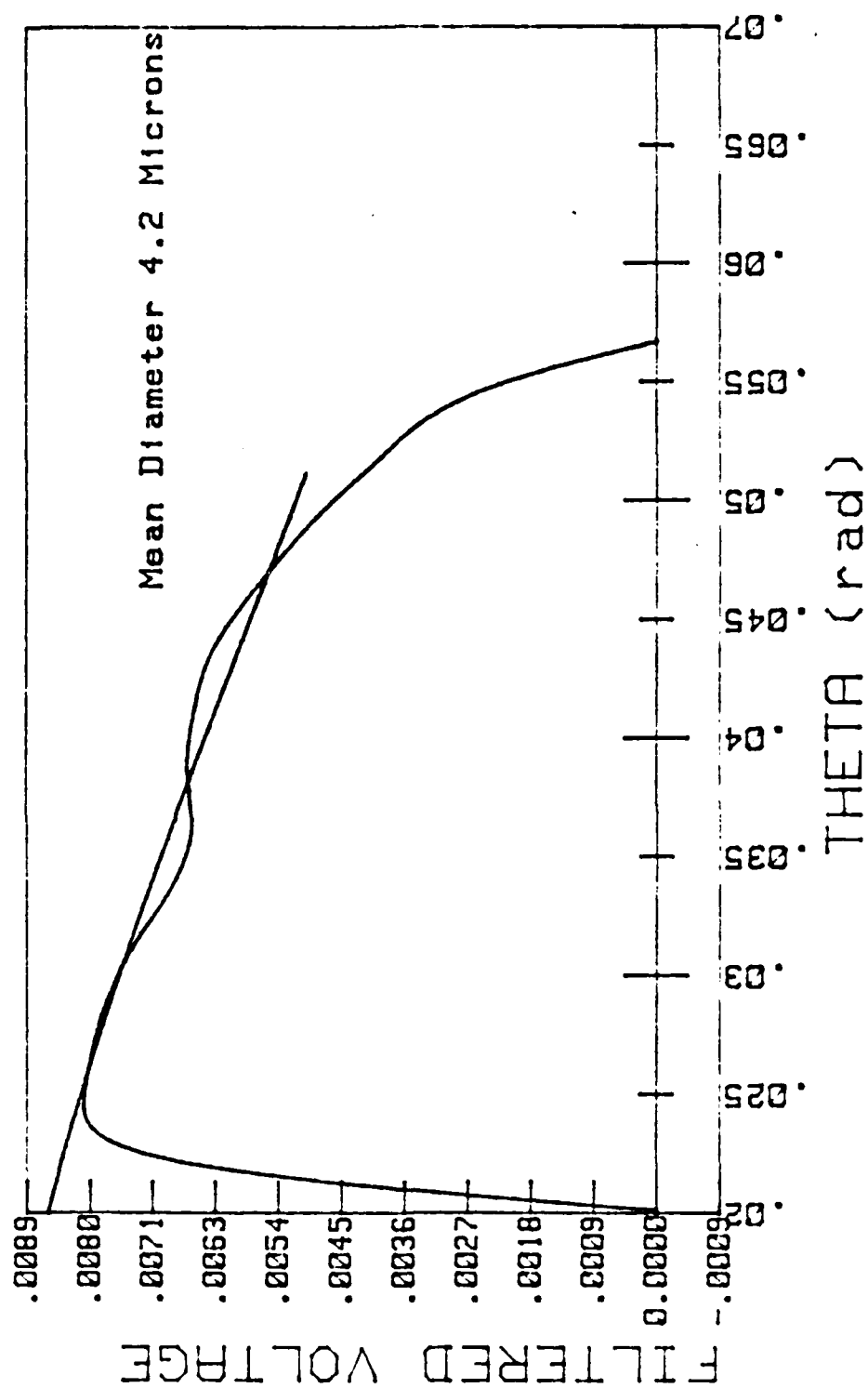
Figure 4.10   Calibration with 4.5 Micron Polystyrene Spheres.
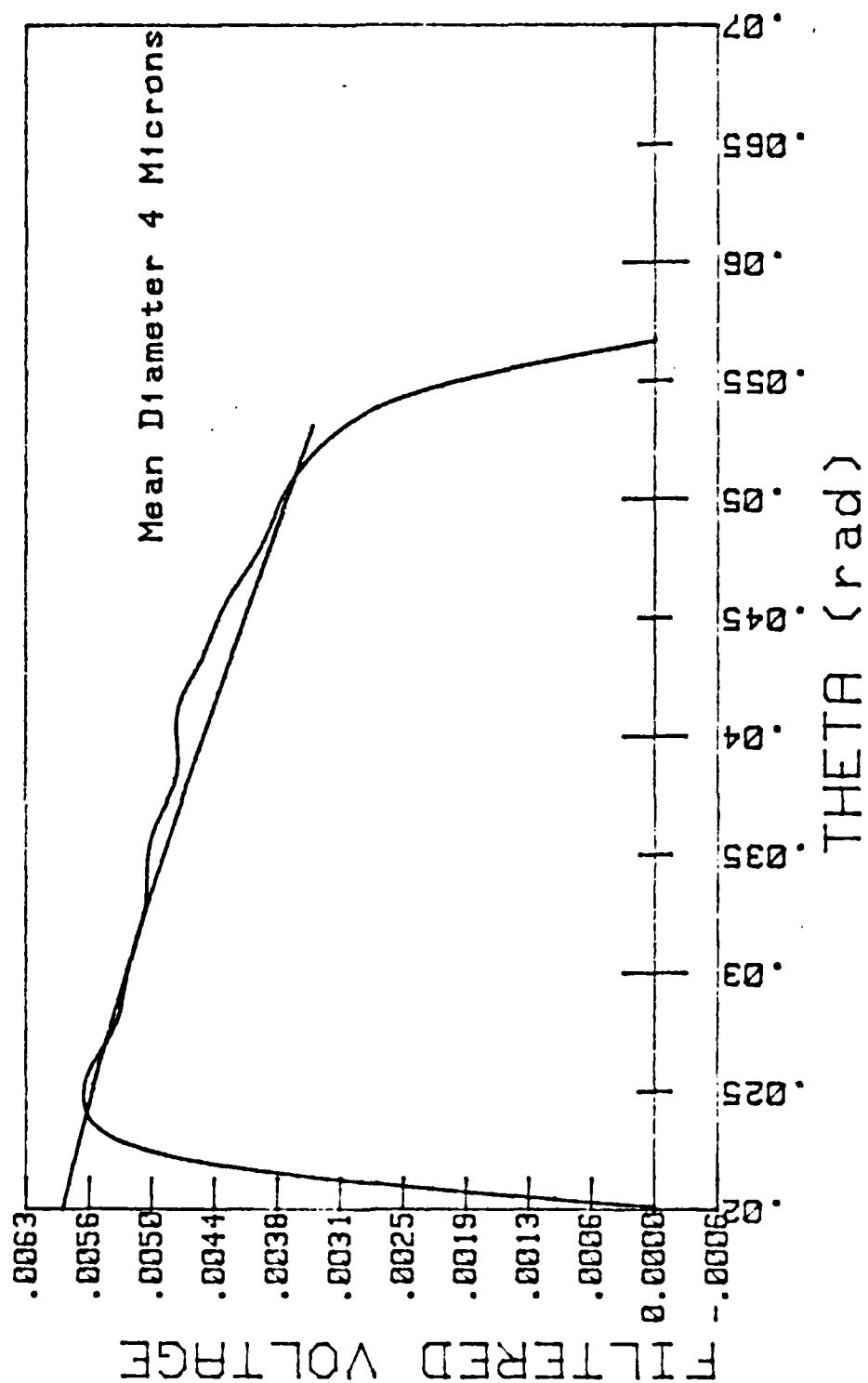
Figure 4.11   Calibration with 4.5 and 0.9 Micron
Polystyrene Spheres.

43

TABLE III
SUMMARY OF 25 MICRON GLASS BEADS FIRING

Date of Test	Press Pr (psig)	Press Max Pc (psig)	Motor D_{32} (microns)	Exhaust D_{32} (microns)	Residence Time (sec)
1 May	320	350	21	13	.092
2 May	275	310	22	18	.092
3 May	600	600	24	22	.091

Notes: Calculated D_{32} (SEM) of 25 microns.

Measured D_{32} (light scattering) of 24 microns.

Pressure column labeled Pr indicates pressure at which data was taken.
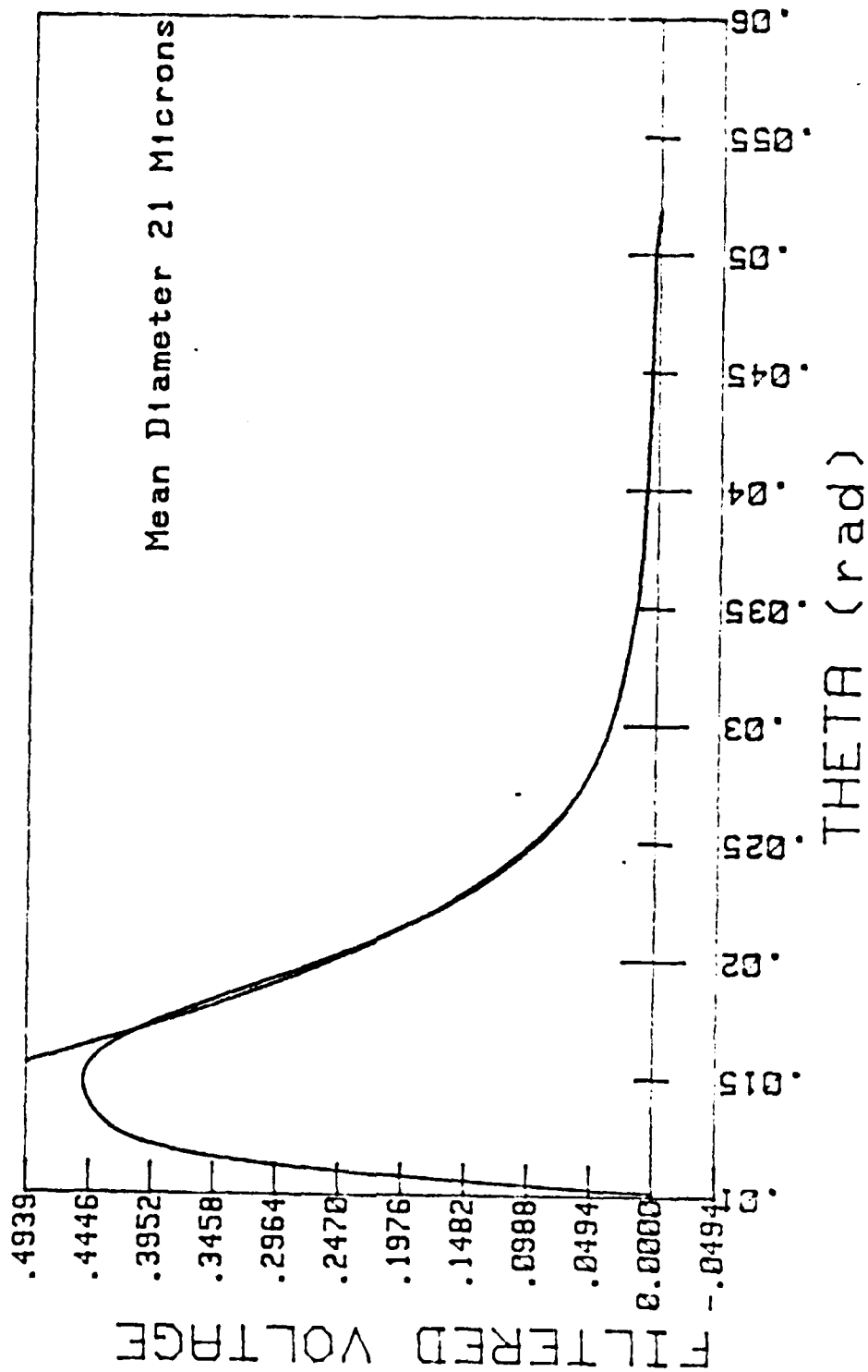
Figure 4.12   Motor Curve Fit - 1 May.
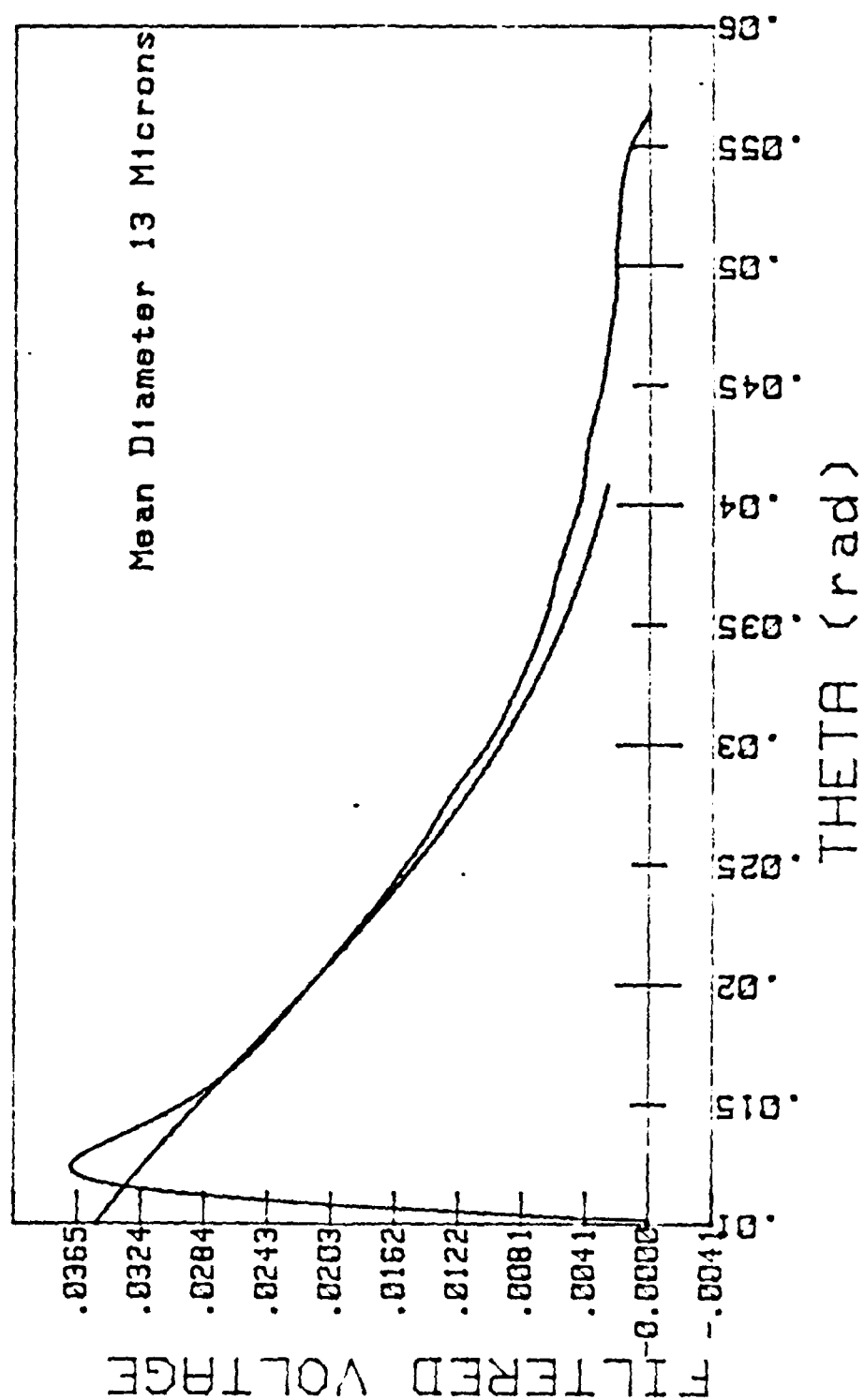
Figure 4.13   Exhaust Curve Fit - 1 May.

46
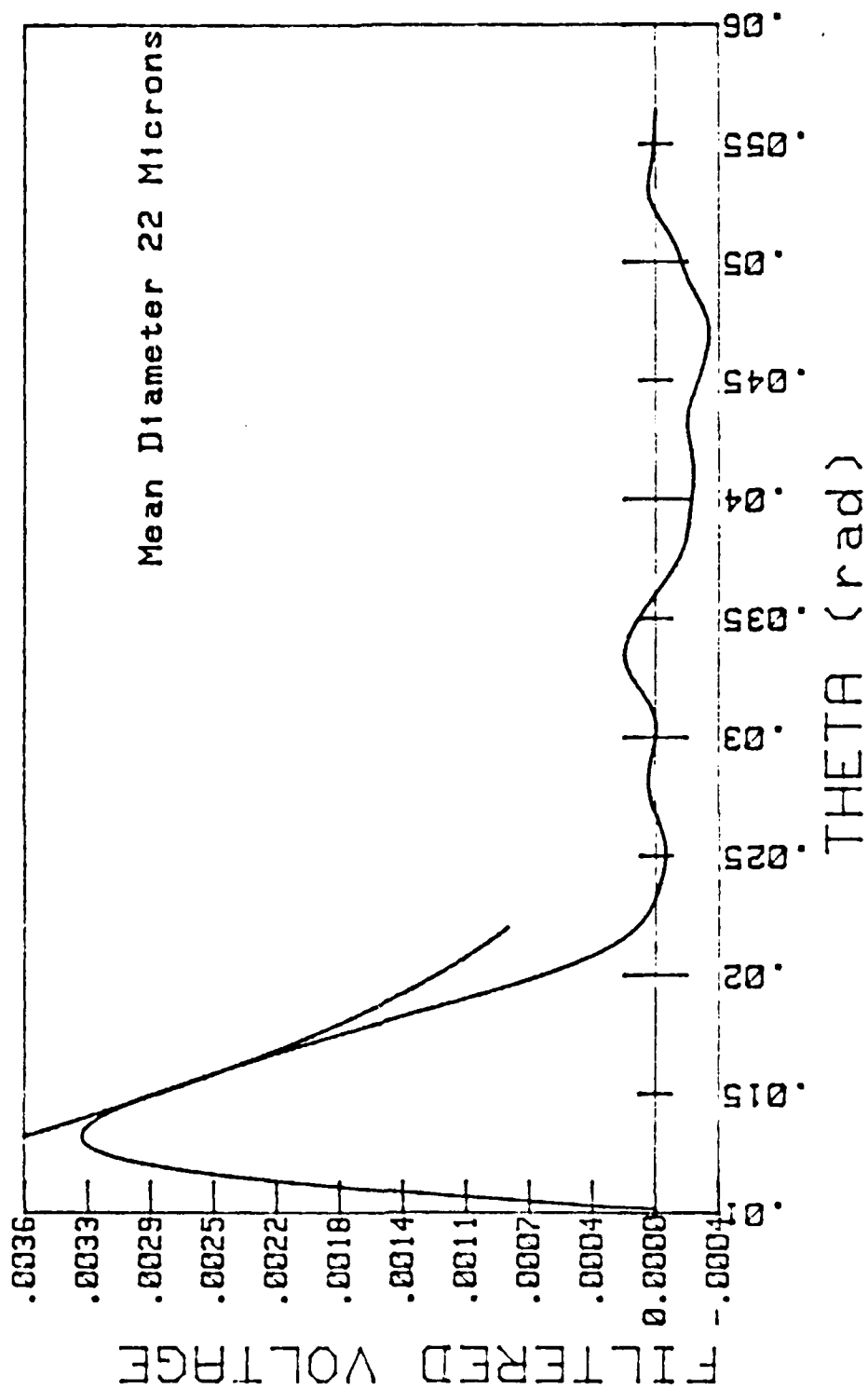
Figure 4.14   Motor Curve Fit - 2 May.

47
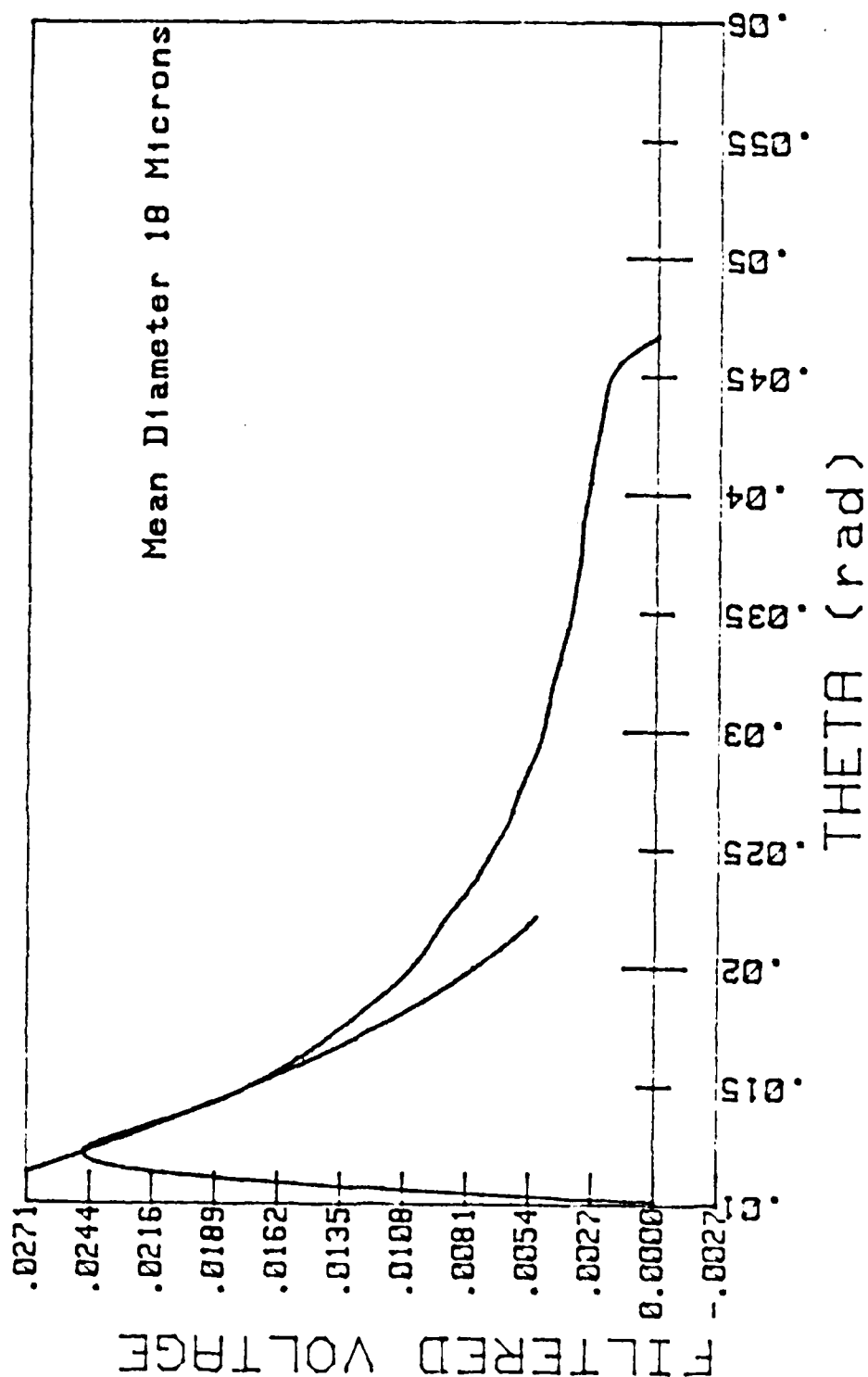
Figure 4.15   Exhaust Curve Fit - 2 May.
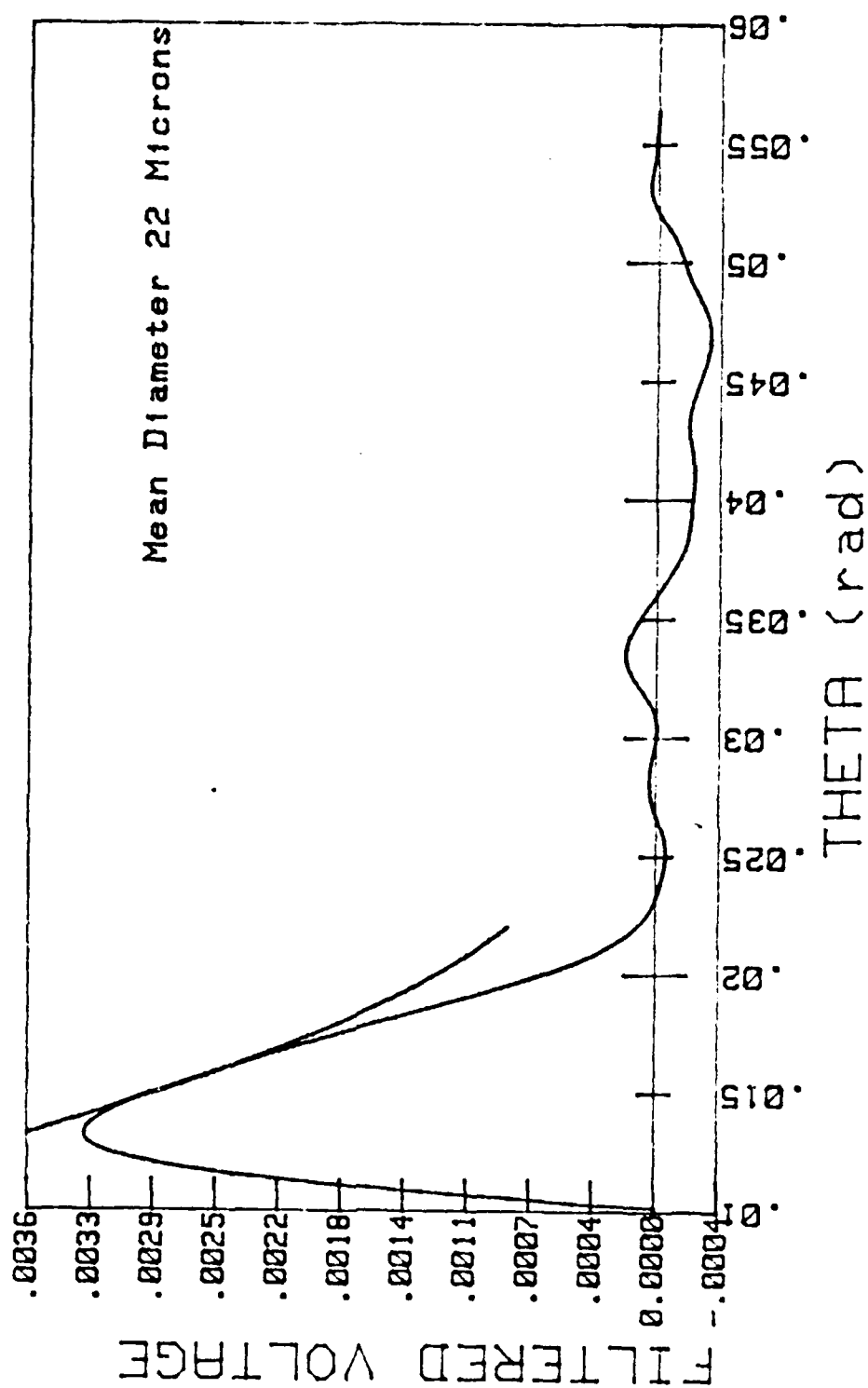
48
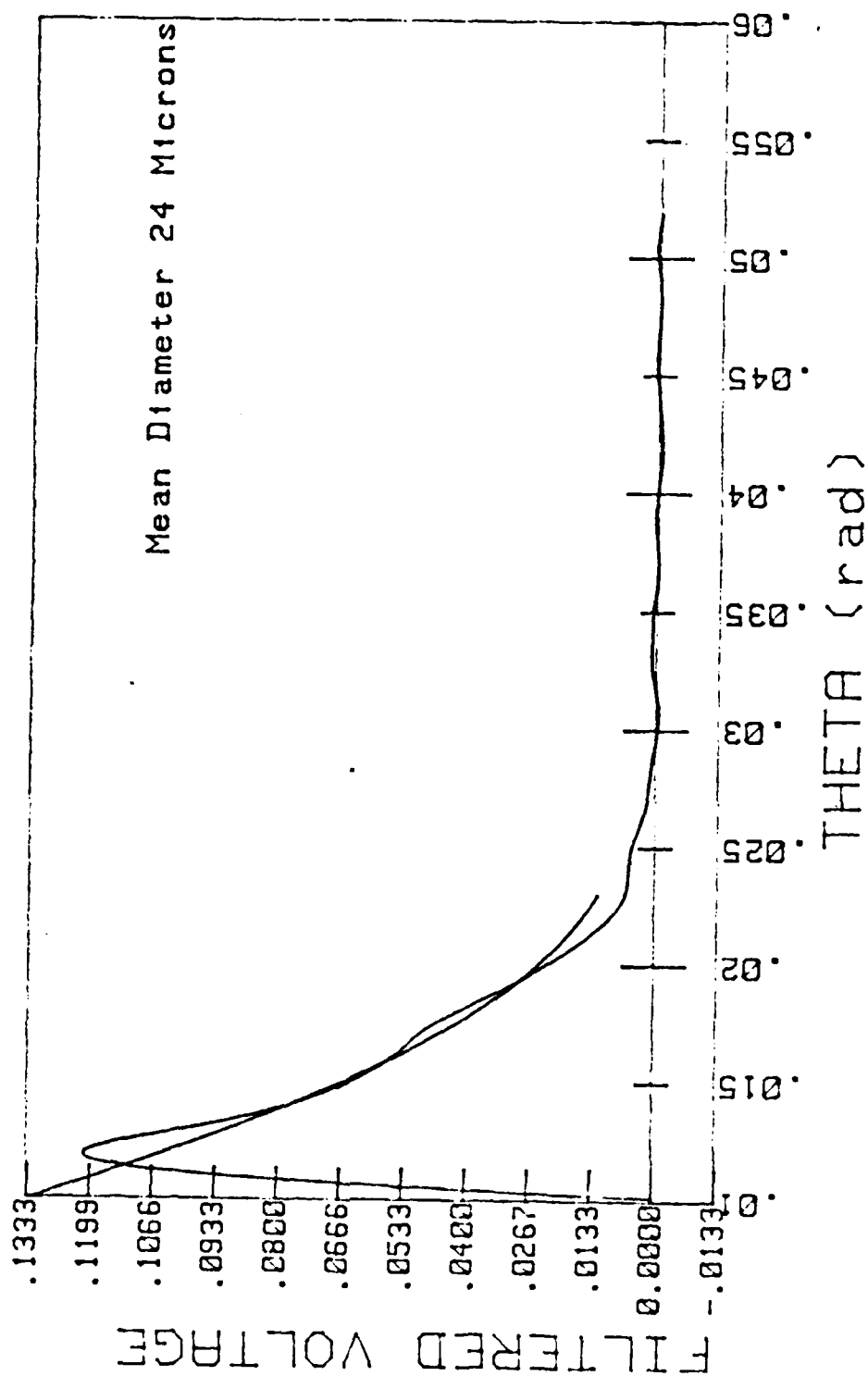
Figure 4.16   Motor Curve Fit - 3 May.

Figure 4.17   Exhaust Curve Fit - 3 May.

50

TABLE IV

SUMMARY OF LIGHT SCATTERING DATA FOR ALUMINUM OXIDE FIRINGS

Date of Test	Press Pr (psig)	Press Max Pc (psig)	Motor D_{32} (Microns)	Exhaust D_{32} (Microns)	Calibration D_{32} (Microns)
25 Apr	(-)	(-)	29	33	(-)
27 Apr	220	430	(-)	30	(-)
4 May	290	315	23	18*	22
5 May	335	420	21	25	23
6 May	260	285	20	25	22
8 May	390	500	22	28	25

Notes: (-) indicates sample not taken or data not obtain

* profile obtained in last scan of exhaust and is lower for this reason

TABLE V

SUMMARY OF SEM DATA FOR ALUMINUM OXIDE FIRINGS

Date of Test	Sample D_{32} (microns)	Nozzle* D_{32} (microns)	Exhaust** D_{32} (Microns)	Calculated Mass Flows Particles	Motor Gas
25 Apr	(-)	(-)	(-)	3.0	(-)
27 Apr	(-)	(-)	(-)	1.9	61
4 May	28	31.5	33	1.9	44
5 May	27.3	31	34	1.9	59
6 May	29	35	31	1.9	40
8 May	(-)	31.5	34.5	1.9	71

Notes: Mass flow for alluminum oxide and propellant are in lb/sec 10^{-3}.

* particles collected from nozzle face.

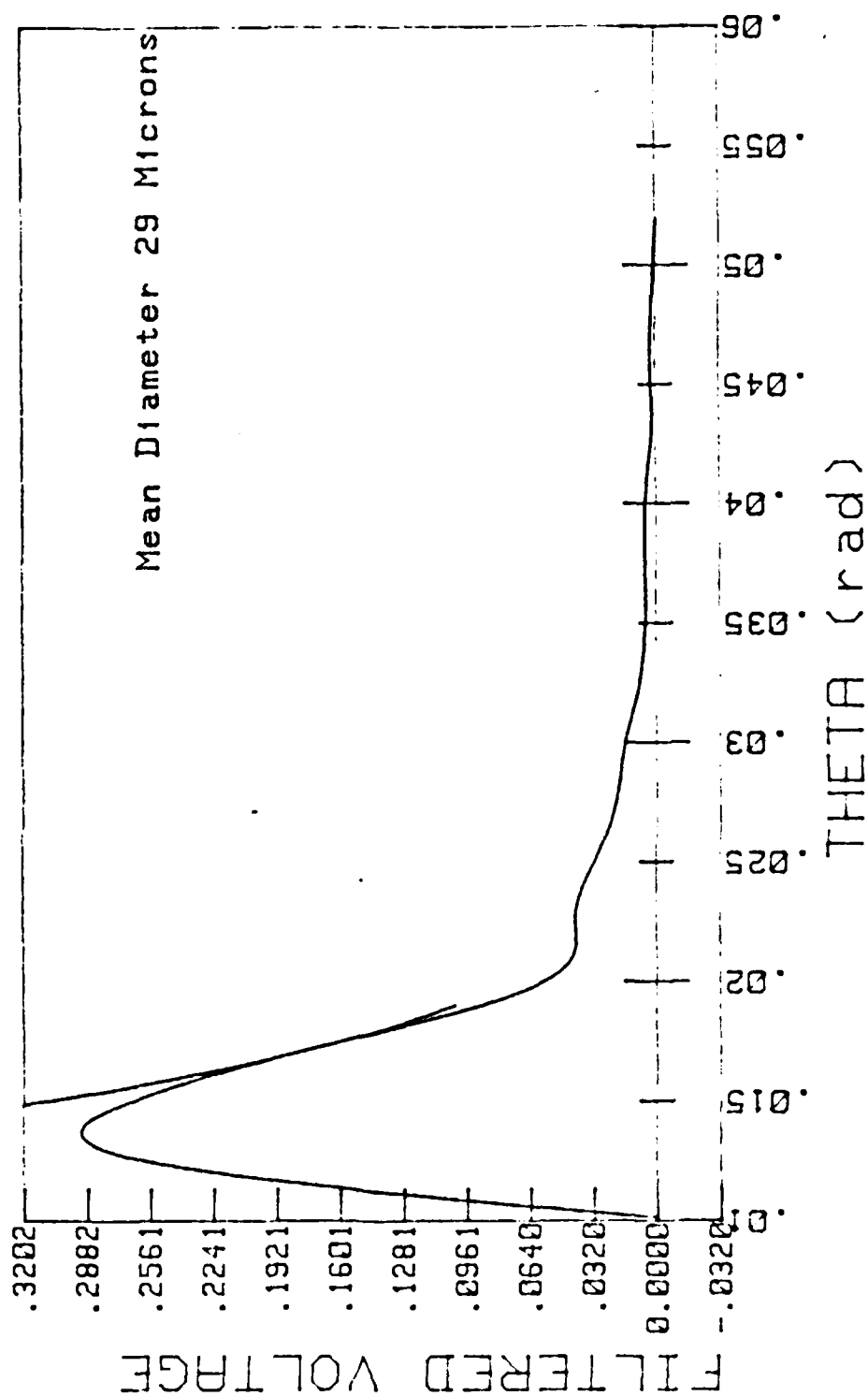** particles collected from exhaust tube.

CURVE FIT RESULTS
INTENSITY vs. THETA

Mean Diameter 29 Microns

Figure 4.18   Motor Curve Fit - 25 April.
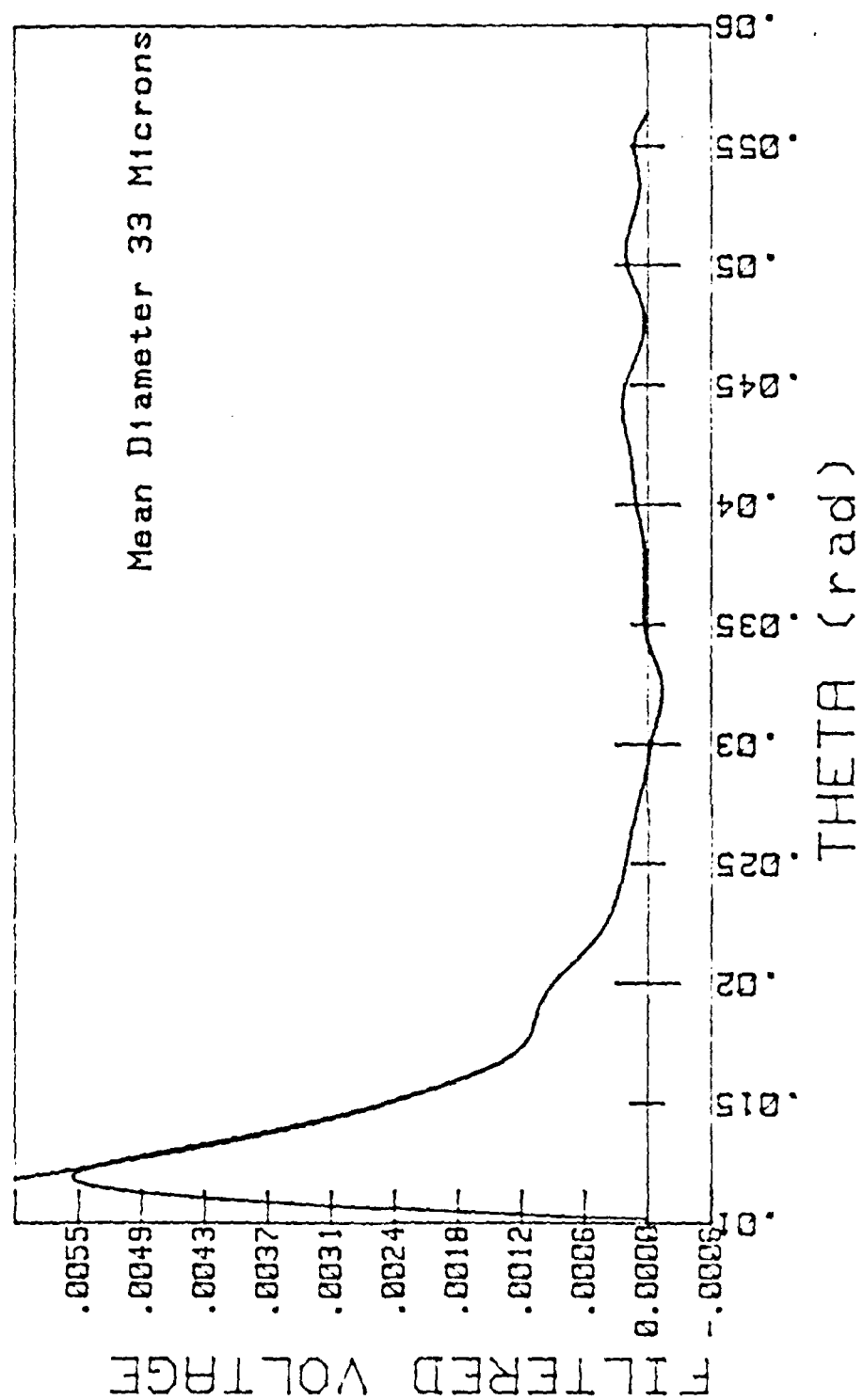
Figure 4.19   Exhaust Curve Fit - 25 April.

53
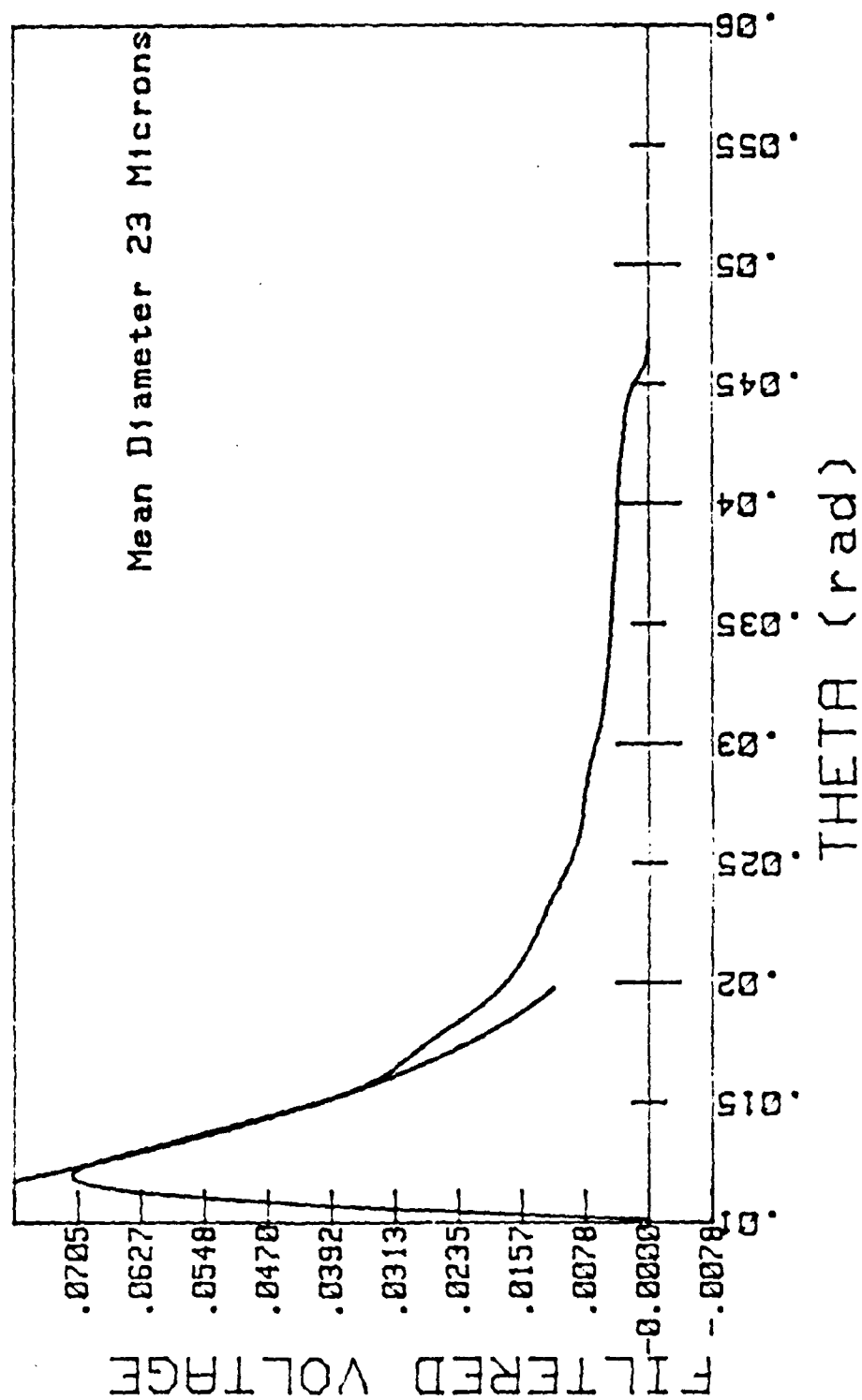
Figure 4.20   Motor Curve Fit - 4 May.
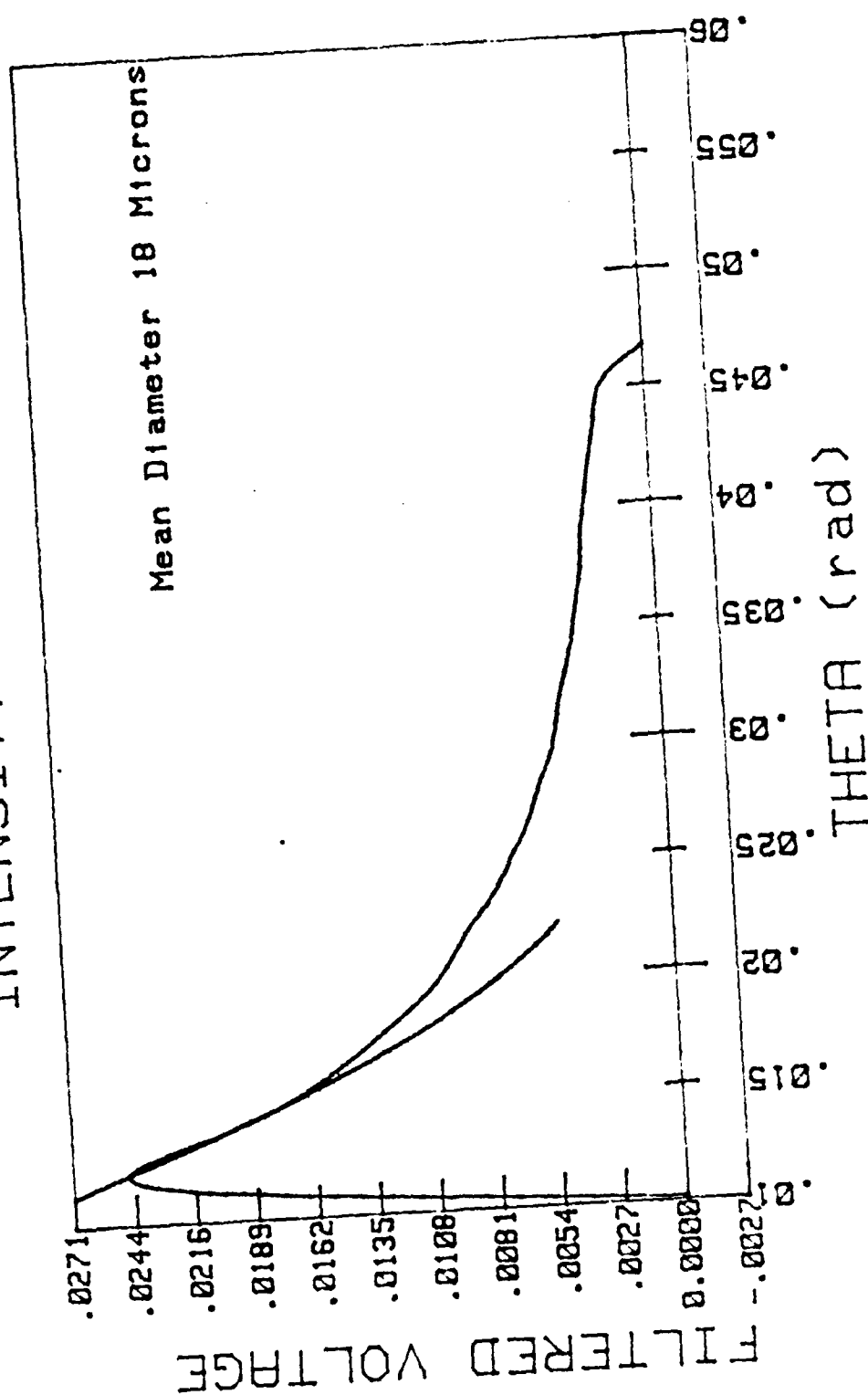
Figure 4.21   Exhaust Curve Fit - 4 May.

55
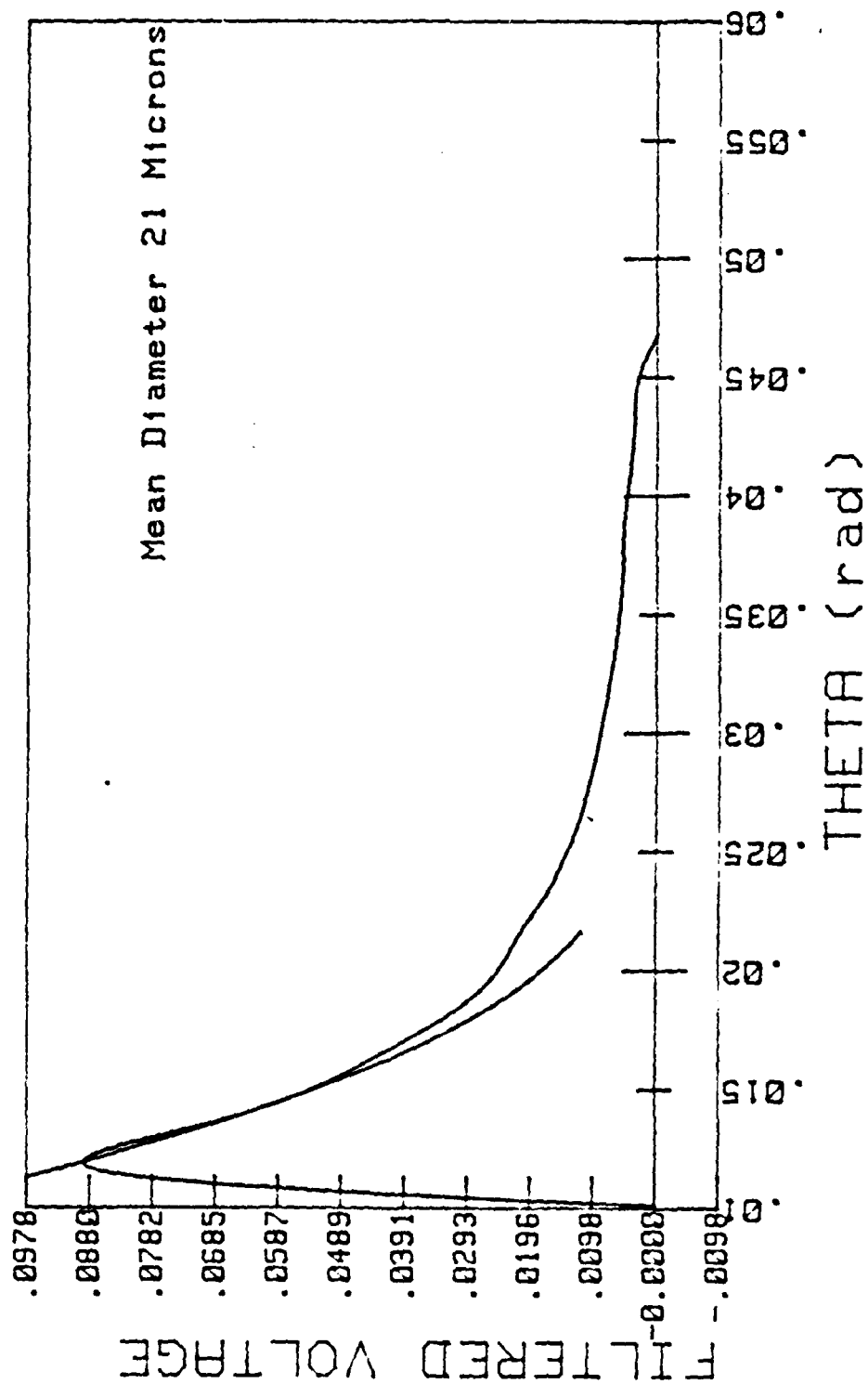
Figure 4.22   Motor Curve Fit - 5 May.

56

Figure 4.23   Exhaust Curve Fit - 5 May.

57

Figure 4.24   Motor Curve Fit - 6 May.

58
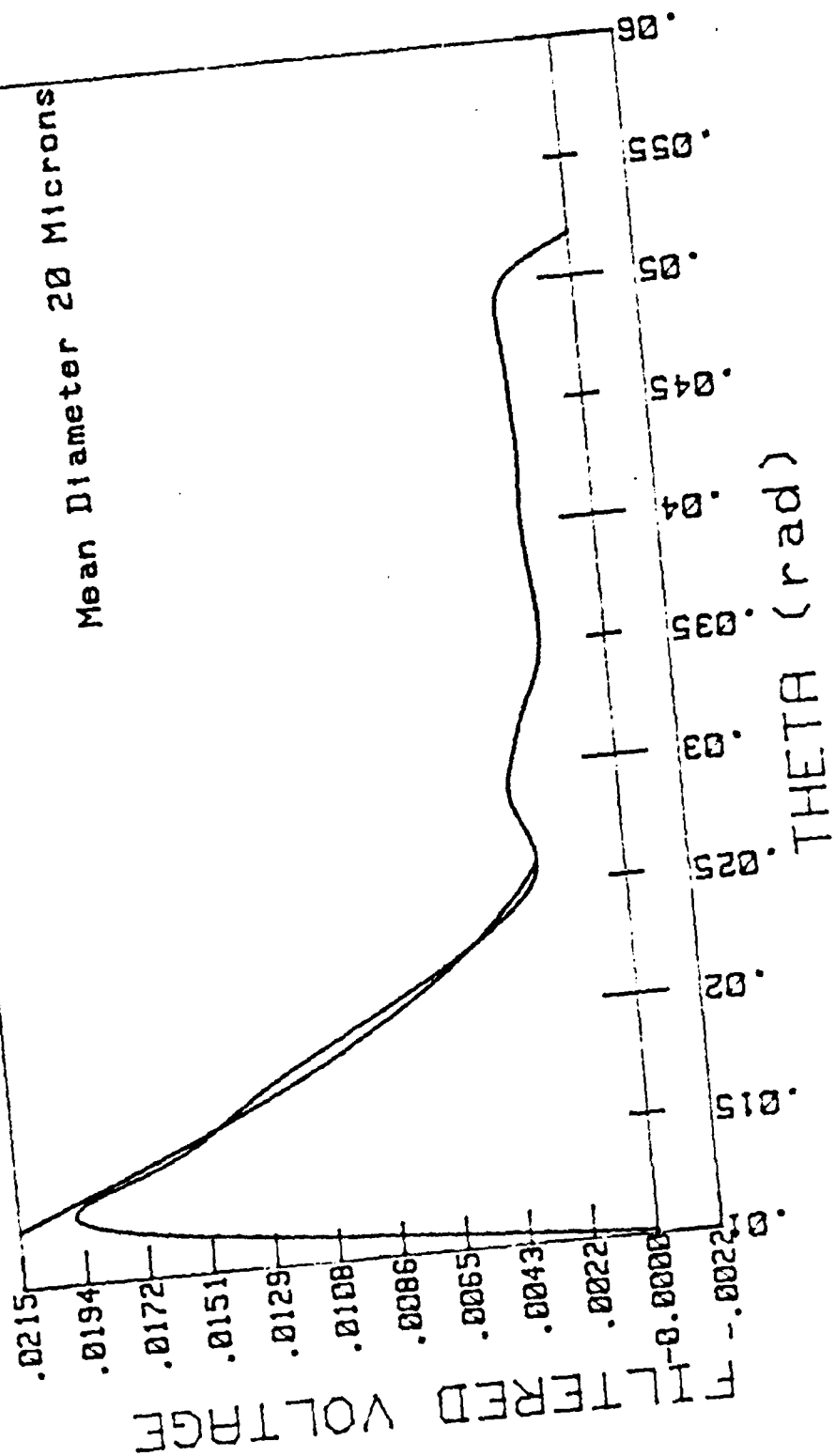
Figure 4.25   Exhaust Curve Fit - 6 May.

CURVE FIT RESULTS
INTENSITY vs. THETA

Mean Diameter 22 Microns
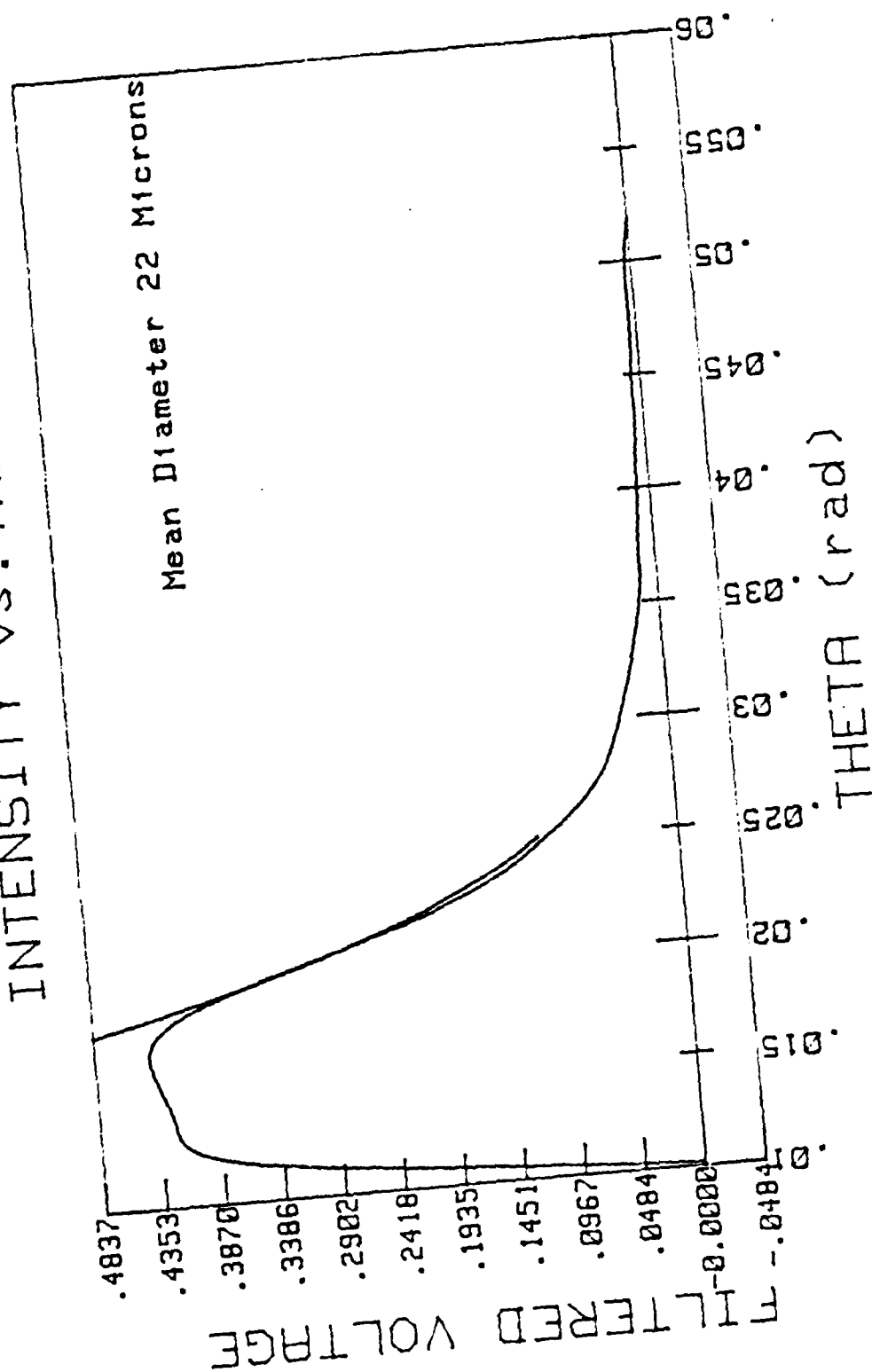
Figure 4.26   Motor Curve Fit - 8 May.

60

Figure 4.27   Exhaust Curve Fit - 8 May.

TABLE VI
THEORETICAL RESIDENCE TIMES

Press (psig)	Propellant	Windows	Nozzle Throat
250	.00028	.049	.09
400	.00027	.049	.09
600	.00027	.048	.09

Note: All times in seconds.

V. CONCLUSIONS AND RECOMMENDATIONS

The results of this investigation have shown that the measurement of D_{32} across the exhaust nozzle when particles of a known mean diameter are fed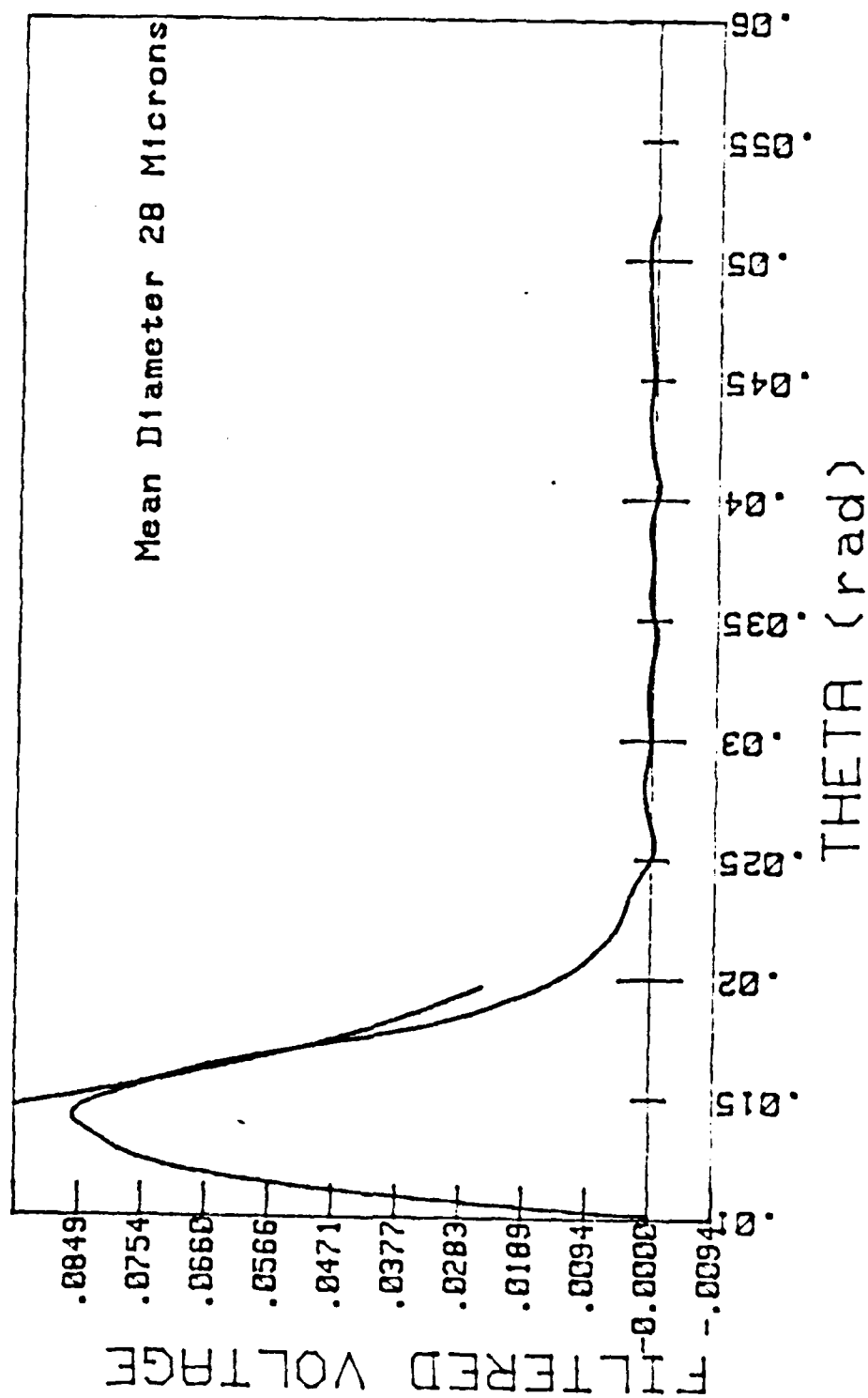 into the motor is possible. However, further development and use of the present apparatus is restricted to the availability of small (1 to 20 microns) spherical metal particles.

Subsequent work should consider the employment of a larger (dimensional cross-section) rocket motor to enable the investigator to reduce, and hopefully eliminate particle impingement on the propellant surface. This modification would allow the rocket motor chamber pressure to be under the control of the investigator through variation of the nozzle throat diameter.

The present optical system and propellant in use provided good data with minimal noise and combustion light interference with the photodiode arrays. One apparatus change that could be adopted would be the modification of the small window port of the motor to accept a larger window. This alteration would not adversely effect the internal gas flow in the motor, but would eliminate the sidewall diffraction and noise periodically encountered with the small window, and greatly ease the apparatus set up and post-fire cleaning.

It is recommended that the present apparatus and propellant be used to create a data base for various metal additives. Simply, different additives, of known D_{32}, could be introduced into the rocket motor using the present set up and relative information about their behavior and life sequence could be determined and used towards improving model prediction codes. Possible metals for consideration would be aluminum, magnesium, zirconium, and boron.

63

LIST OF REFERENCES

1. Air Force Rocket Propulsion Laboratory Report 75-36, Volume 1, *A Computer Program for the Prediction of Solid Propellant Rocket Motor Performance*, by D.E. Coats, et al., July 1975.

2. Air Force Rocket Propulsion Laboratory Interim Report 80-34, Volume 1, *A Computer Program for the Prediction of Solid Propellant Rocket Motor Performance*, by D.E. Coats, G.R. Nickerson, and R.W. Hermsen, et al., April 1981

3. Hermsen, R.W. "Aluminium Oxide Particle Size for Solid Rocket Motor Performanc Predictions," AIAA 19th Aerospace Sciences Meeting, St Louis, Missouri, January 12-15, 1981.

4. Price, E.W., "Combustion of Metalized Propellants," *Progess in Astronautics and Aeronautics*, Volume 90, pp.479-505, 1984.

5. Harris, R.K., *An Apparatus for Sizing Particulate Matter in Solid Rocket Motors*, M.S. Thesis, Naval Postgraduate School, Monterey, California, 1983.

6. Kertadidjaja, A., *Particle Sizing in a Solid Rocket Motor Using the Measurement of Scattered Light*, M.S. Thesis, Naval Postgraduate School, Monterey, California, 1985.

7. Buchele, D.R., "Particle Sizing by Measurement of Forward Scattered Light at Two Angles," *Nasa Technical Paper 2156*, May 1983.

8. Rosa, J.S., *Particle Sizing in a Solid-Propellant Rocket Motor Using Scattered Light Measurements*, M.S. Thesis, Naval Postgraduate School, Monterey, California, 1985.

9. Van de Hulst, H.C., *Light Scattering by Small Particles*, John Wiley and Sons, Inc., New York, 1957.

10. Dobbins, R.A., Crocco, L. and Glassman, I., "MeasureMent of MeanParticle Sizes of Spraysfrom Diffractively Scattered Light," *AIAA Journal*, v.1, No.8, pp.1882-1886, 1963.

11. Mugele, R.A. and Evans, H.D., "Droplet Size Distribution in Sprays," *Industrial and Engineering Chemistry*, v.43, pp.1317-1324, 1951.

INITIAL DISTRIBUTION LIST

		No. Copies
1.	Defense Technical Information Center Cameron Station Alexandria, Virginia 22304-6145	2
2.	Library, Code 0142 Naval Postgraduate School Monterey, California 93943-5002	2
3.	Department Chairman, Code 67 Department of Aeronautics Naval Postgraduate School Monterey, California 93943-5000	1
4.	Professor D.W. Netzer, Code 67 Nt Department of Aeronautics Naval Postgraduate School Monterey, California 93943-5000	2
5.	Director Land Armament and Electronics Engineering and Maintenance National Defence Headquarters Ottawa, Ontario Canada K1A OK2	1
6.	Director Personnel Education and Development National Defence Headquarters Ottawa, Ontario Canada K1A OK2	1
7.	Captain K.G. Horton Directorate of Land Armament and Electronics Engineering and Maintenance 4-6 National Defence Headquarters Ottawa, Ontario Canada K1A OK2	2